

Terraforming Mars: Mass, Forcing, and Industrial Throughput Constraints

Slava G. Turyshev

*Jet Propulsion Laboratory, California Institute of Technology,
4800 Oak Grove Drive, Pasadena, CA 91109-0899, USA*

(Dated: March 3, 2026)

Terraforming Mars can be evaluated with a small set of system-level feasibility constraints linking (i) target pressures and compositions to required atmospheric inventories, (ii) target surface temperatures to required radiative control authority (TOA forcing and/or effective longwave opacity), (iii) inventories and radiative agents to sustained industrial throughput and power over a build time, and (iv) persistence against collapse, escape, and geochemical sinks. We use transparent order-of-magnitude scalings to map proposed levers (endogenous CO₂ release, synthetic super-greenhouse gases, CO₂-H₂ CIA, engineered aerosols/nanoparticles, orbital mirrors/albedo modification, and regional solid-state greenhouse “paraterraforming”) onto common metrics $\{M, \tau_{\text{IR}}/\Delta F_{\text{TOA}}, \dot{M}, P\}$. We find: (1) human-relevant pressures imply exaton-class inventories, $M_{\text{atm}} \simeq 4\pi R_{\text{Mars}}^2 P_s / g_{\text{Mars}} \sim 10^{17}$ – 10^{18} kg; (2) accessible CO₂ plausibly provides $\lesssim 20$ mbar, yielding $\lesssim 10$ K warming under present insolation; (3) achieving $T_s \sim 250$ – 273 K at current insolation requires an effective IR opacity target $\tau_{\text{IR,eff}} \sim 2$ – 4 (uncertain at the ~ 30 – 50% level but not altering mass-scale conclusions); and (4) breathable endpoints are dominated by O₂ and buffer-gas mass and by a minimum oxygenation work $\gtrsim 10^{25}$ J, implying $\dot{M} \sim 10^7$ – 10^8 kg s⁻¹ and multi- 10^2 TW to PW-class average power for century-to-millennial build times (before inefficiencies and sink filling). We conclude that regional habitability gains via paraterraforming are plausible on near-term industrial scales, whereas global transformation of Martian environment requires multi-century planetary industry and becomes credible only under conditions of (a) massive exogenous volatile supply or much larger discovered inventories, and (b) sustained high-authority climate control and retention against sinks and loss.

I. INTRODUCTION

Terraforming Mars denotes deliberate, sustained modification of Mars’ surface environment—atmospheric pressure and composition, radiative balance, and water stability—toward states that support progressively less technologically mediated surface habitability. The concept is widely discussed, but feasibility is governed by a compact set of planet-scale feasibility constraints that any proposed pathway must satisfy simultaneously.

We use four governing constraints as a common quantitative basis for comparing mechanisms: (i) *mass inventory constraint*, linking target pressures and partial pressures to required volatile inventories; (ii) *radiative-balance constraint*, linking target surface temperatures to required top-of-atmosphere (TOA) forcing ΔF_{TOA} and/or effective longwave optical depth τ_{IR} ; (iii) *throughput-and-power constraint*, linking inventories and radiative agents to required sustained throughput \dot{M} and power P over specified build times; and (iv) *stability/retention constraint*, requiring persistence against atmospheric collapse/condensation, escape to space, and geochemical sequestration. These simplified scalings are intentionally simple: they provide optimistic order-of-magnitude bounds that expose dominant bottlenecks and feasibility floors. Table I provides a list of acronyms used here.

This paper is an engineering-level synthesis. We avoid black-box climate and trajectory solvers and instead use transparent scalings to map proposals onto common, reviewer-auditable metrics $\{M, \tau_{\text{IR}}/\Delta F_{\text{TOA}}, \dot{M}, P\}$. The results are therefore lower bounds and feasibility discriminators, not predictions of a specific Mars climate state; quantitative state prediction requires coupled 3-D GCM, aerosol microphysics, and photochemical/geochemical cycling.

Classic terraforming treatments [1–3] introduced key concepts and qualitative feasibility arguments. More recent work has provided strong constraints and mechanism-specific quantification, including limits on accessible CO₂ inventories [4], regional solid-state greenhouse paraterraforming [5], and engineered aerosol warming proposals [6]. The contribution here is not a new warming mechanism; it is a unified systems/architecture trade framework that (a) keeps the governing constraints explicit and (b) reduces disparate proposals to common quantitative requirements in mass, forcing/opacity, throughput, and power. This framing highlights which constraint dominates for a given end state and makes key uncertainties (e.g., accessible nitrogen inventory, aerosol lifetimes, and sink capacities) explicit.

Three quantitative facts motivate our constraint-based framework. First, accessible CO₂ reservoirs are plausibly limited to $\mathcal{O}(10$ – 20 mbar), yielding $\lesssim 10$ K warming under present insolation [4]. Second, mechanisms with high radiative leverage at low added atmospheric mass (e.g., aerosols or H₂ CIA) generally translate into sustained replenishment and power requirements [6]. Third, breathable endpoints are dominated by the required masses of O₂ and buffer gas (N₂/Ar) and by $\gtrsim 10^{25}$ J-class minimum energy requirements for oxygen production even at reversible limits.

This paper is organized as follows: Section II defines end states (E0–E4) and baseline Mars parameters. Section III

TABLE I. Acronyms used in this paper.

Acronym	Meaning
CIA	collision-induced absorption
GCM	general circulation model
IR	infrared
ISRU	in-situ resource utilization
LW	longwave
PFC	perfluorocarbon (super-greenhouse gas class)
PV	photovoltaics
SW	shortwave
TOA	top-of-atmosphere

develops atmospheric mass bookkeeping and buffer gas requirements. Section IV establishes radiative requirements, including a minimal greenhouse mapping linking T_e and T_s . Section V bounds what can be achieved by mobilizing endogenous CO_2 and H_2O . Section VI evaluates engineered and exogenous warming options (PFC-class gases, CO_2 - H_2 CIA, engineered aerosols, mirrors/albedo). Section VII quantifies the mass and minimum energy requirements for oxygenation and breathable endpoints. Section VIII discusses loss, collapse, and sequestration constraints. Section IX synthesizes energy delivery and system architecture as a coupled control problem. Section X discusses implications, industrial scaling, timescale–power trade, and cost floors; and Section XI concludes.

II. WHAT “TERRAFORMING MARS” MEANS IN QUANTITATIVE TERMS

A. End states and success metrics

The term *terraforming* is used inconsistently. For technical analysis it is useful to define explicit end states with measurable criteria:

- E0: “*Robotic/human assisted operations*” (*today*). Current mean $P_s \sim 610$ Pa and $T_s \sim 210$ K, requiring pressure suits and thermal control.
- E1: “*Water metastability*”. A minimum criterion is P_s above the triple-point pressure of water, $P_s > 611.657$ Pa at 273.16 K [7], plus episodic surface temperatures above freezing in some regions. This criterion is frequently misunderstood: exceeding the triple point is necessary but far from sufficient for stable surface liquid water (Sec. IV C).
- E2: “*Open-air agriculture / shirtsleeve greenhouses*”. A pragmatic criterion is $P_s \gtrsim 10$ kPa with greenhouse structures providing the remaining pressure/thermal margins. This reduces structural loads by $\sim 10\times$ compared to 101 kPa.
- E3: “*Unsuited human exposure without ebullism*”. To prevent boiling of body fluids at 37°C , vehicle and habitat standards require total pressure $P_s \geq 6.27$ kPa (the Armstrong limit) [8]. This is a lower bound; hypoxia, CO_2 toxicity, and decompression sickness impose stricter requirements on composition and partial pressures.
- E4: “*Breathable, Earth-like*”. A common benchmark is $p_{\text{O}_2} \sim 21$ kPa with a buffer gas (N_2/Ar) to reach $P_s \sim 50$ – 100 kPa and to control fire risk and physiology. This endpoint is dominated by the required mass of O_2 and buffer gases (Sec. VII).

Classic terraforming proposals and feasibility discussions span several decades and include early quantitative treatments of Mars warming and atmospheric engineering [1–3]. This paper emphasizes the distinction between (i) *global atmospheric modification* and (ii) *regional/paraterraforming* strategies that create habitable microclimates without altering planetary-scale atmospheric mass.

We use representative mean values (Table II) for Mars physical and radiative parameters. Solar irradiance at Mars varies substantially between perihelion and aphelion; we use the orbit-averaged top-of-atmosphere (TOA) value $S_{\text{Mars}} \approx 589 \text{ W m}^{-2}$ and a mean planetary albedo $A_B \approx 0.25$ [9]. These yield an effective radiating temperature $T_{e0} \approx 210$ K, consistent with Mars’ cold climate.

TABLE II. Nominal Mars parameters used in first-order calculations.

Quantity	Symbol	Value
Mean radius	R_{Mars}	3389.5 km
Surface gravity	g_{Mars}	3.71 m s^{-2}
Surface area	$4\pi R_{\text{Mars}}^2$	$1.44 \times 10^{14} \text{ m}^2$
Mean TOA solar irradiance	S_{Mars}	589 W m^{-2}
Bond albedo (mean)	A_{B}	~ 0.25
Effective radiating temperature	$T_{\text{e}0}$	$[S_{\text{Mars}}(1 - A_{\text{B}})/(4\sigma_{\text{SB}})]^{1/4} \approx 210 \text{ K}$

TABLE III. Pressure endpoints and implied global atmospheric inventories on Mars. Atmospheric mass uses $M_{\text{atm}} \simeq (4\pi R_{\text{Mars}}^2/g_{\text{Mars}})P_s$ from Eq. (1) and column mass uses $m_{\text{col}} = P_s/g_{\text{Mars}}$. Note: 1 bar shown as a convenient Earth sea-level reference.

End state	Meaning	P_s (Pa)	P_s (mbar)	M_{atm} (kg)	m_{col} (kg m^{-2})
E0	Present mean	6.1×10^2	6.1	2.37×10^{16}	1.64×10^2
E1	Water triple point	6.12×10^2	6.12	2.38×10^{16}	1.65×10^2
—	CO ₂ mobilization ceiling	2.0×10^3	20	7.78×10^{16}	5.39×10^2
E3	Armstrong limit (no ebullism)	6.27×10^3	62.7	2.44×10^{17}	1.69×10^3
—	0.2 bar (thick but not Earthlike)	2.0×10^4	200	7.78×10^{17}	5.39×10^3
E4	1 bar (Earth sea-level)	1.0×10^5	1000	3.89×10^{18}	2.70×10^4

B. Key results at a glance

Table III provides pressure endpoints and implied global atmospheric inventories on Mars. Table IV summarizes the requirement targets used throughout this paper as a compact “dashboard” linking end states (E0–E4) to (i) required inventories, (ii) radiative control targets, and (iii) implied industrial rates. This table makes explicit a central theme of the paper: as the endpoint advances from E2 to E4, the dominant constraint shifts from local radiative control and deployment area to exaton-class inventories and multi-century industrial throughput and power.

III. ATMOSPHERIC MASS BOOKKEEPING: PRESSURE TARGETS IMPLY EXATON-SCALE GASES

A. Pressure–mass relation

For a thin atmosphere in hydrostatic equilibrium, the global atmospheric mass required to produce a mean surface pressure P_s is approximately

$$M_{\text{atm}} \simeq \frac{4\pi R_{\text{Mars}}^2}{g_{\text{Mars}}} P_s. \quad (1)$$

Using Table II, the conversion is

$$M_{\text{atm}} \approx 3.89 \times 10^{15} \text{ kg per mbar} \quad (\text{Mars}). \quad (2)$$

Figure 1 plots Eq. (1) over 0.1–1000 mbar.

Table III highlights several pressure endpoints relevant to “success” criteria. The central message is scale: moving from present-day Mars (~ 6 mbar) to even modest human-relevant pressures is an *exaton* (10^{18} kg) class problem.

Also, from Eq. (1), we derive atmospheric mass per unit pressure

$$\frac{dM_{\text{atm}}}{dP_s} = \frac{4\pi R_{\text{Mars}}^2}{g_{\text{Mars}}} \approx 3.89 \times 10^{13} \text{ kg Pa}^{-1} \approx 3.89 \times 10^{15} \text{ kg mbar}^{-1}. \quad (3)$$

B. Composition matters: CO₂ is a poor buffer gas

Pressure targets do not specify composition, but composition determines physiology and climate.

TABLE IV. Requirements dashboard for representative endpoints. Inventories use $M \simeq (4\pi R_{\text{Mars}}^2/g_{\text{Mars}})P$. Radiative targets assume $T_{e0} \approx 210$ K unless noted. Where ranges are shown, they correspond to build times $t_{\text{build}} = 10^3$ yr (left) to 10^2 yr (right). All power numbers are thermodynamic minima unless stated otherwise. \dot{M} assumes global deployment; E2 is typically regional.

End state	Success criterion (global unless noted)	Pressure / p_i	Inventory M [kg]	Radiative/control target	Industrial implication
E0	Current Mars baseline	$P_s \approx 0.611$ kPa (6.1 mbar)	2.37×10^{16}	$T_{e0} \approx 210$ K; $T_s \approx 210$ K	None (baseline)
E1	Water metastability (regional/episodic)	$P_s \gtrsim 0.612$ kPa	$\approx 2.38 \times 10^{16}$	Not globally constrained; local energy balance dominates	Regional heat/insulation; not inventory-limited
E2	Protected agriculture (typically regional)	$P_s \sim 10$ kPa (inside habitats)	—	Local greenhouse insulation control	Deployment area + local power; scalable in phases
E3	No ebullism (Armstrong limit)	$P_s = 6.27$ kPa	2.44×10^{17}	To approach $T_s \gtrsim 250$ K: $\tau_{\text{IR}} \sim 2\text{--}3$ (or high-authority ΔF_{TOA})	If pursued globally: $\dot{M} \sim 7.7 \times 10^6\text{--}7.7 \times 10^7$ kg s ⁻¹ (inventory-limited)
<i>E4 (breathable): inventories + energy dominate; warming still required as in E3.</i>					
E4a	O ₂ partial pressure target	$p_{\text{O}_2} = 21$ kPa	8.2×10^{17}	Warm branch + sink management (Sec. VIII D)	$\dot{M}_{\text{O}_2} \sim 2.6 \times 10^7\text{--}2.6 \times 10^8$ kg s ⁻¹ ; $\bar{P}_{\text{min}} \sim 0.38\text{--}3.8$ PW
E4b	Buffer gas example	$p_{\text{N}_2} = 50$ kPa	1.9×10^{18}	Inventory (climate-independent)	$\dot{M}_{\text{N}_2} \sim 6.0 \times 10^7\text{--}6.0 \times 10^8$ kg s ⁻¹ ; if exogenous, momentum/transport dominates

Notes: (a) If $P_s \sim 10$ kPa were applied *globally*, Eq. (1) implies $M_{\text{atm}} \approx 3.9 \times 10^{17}$ kg; E2 is typically implemented regionally (paraterraforming/habitats), so global inventory is not required. (b) E3 is a pressure-only threshold; human habitability additionally requires low p_{CO_2} and a buffer gas plus p_{O_2} (treated explicitly in E4).

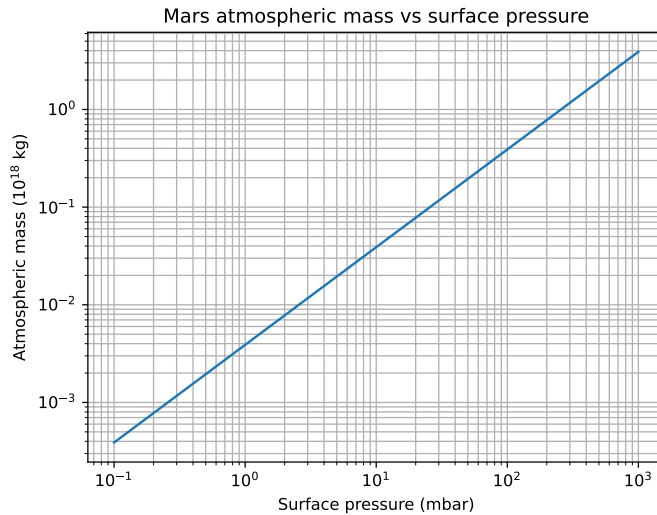


FIG. 1. Atmospheric mass required for a given mean surface pressure on Mars from Eq. (1). A 1 bar atmosphere corresponds to $M_{\text{atm}} \approx 3.89 \times 10^{18}$ kg.

1. CO₂ toxicity constraint.

High CO₂ partial pressures are directly hazardous to humans and many plants. Therefore, even if CO₂ is the primary available endogenous greenhouse gas, a breathable endpoint cannot consist of “CO₂ + O₂” alone at tens of

kPa. A viable E3/E4 atmosphere requires a buffer gas (N₂ and/or Ar) at the tens of kPa level.

2. Available buffer gas on Mars.

Mars' present atmosphere is $\sim 95\%$ CO₂ with minor N₂ and Ar. Scaling these minors to tens of kPa requires either (i) importing buffer gas from external sources or (ii) mining and releasing geochemically stored nitrogen (nitrates, ammonium minerals) if sufficient inventories exist (uncertain at planetary scale). This is a first-order roadblock for E4.

C. Column mass as a proxy for radiation and aerodynamic shielding

Atmospheric column mass is $m_{\text{col}} = P_s/g_{\text{Mars}}$. This quantity is relevant to (i) attenuation of energetic particles and UV (qualitatively), and (ii) aerodynamic effects such as wind stress and parachute/aerobraking performance. For representative endpoints:

$$m_{\text{col}} \approx 2.7 \times 10^3 \text{ kg m}^{-2} \left(\frac{P_s}{10 \text{ kPa}} \right), \quad (4)$$

so $P_s = 6.27 \text{ kPa}$ (Armstrong limit) corresponds to $m_{\text{col}} \approx 1.7 \times 10^3 \text{ kg m}^{-2}$, while $P_s = 101 \text{ kPa}$ corresponds to $m_{\text{col}} \approx 2.7 \times 10^4 \text{ kg m}^{-2}$ on Mars (because $g_{\text{Mars}} < g_{\oplus}$). Thus pressure-building strategies also directly modify shielding and entry/descent regimes, even before composition is made breathable.

D. Buffer gas mass scales and import energetics

A breathable E3/E4 atmosphere requires a *buffer gas* (typically N₂ and/or Ar) at tens of kPa. The mass requirement follows directly from Eq. (1). For example, targeting $p_{\text{N}_2} = 50 \text{ kPa}$ implies

$$M_{\text{N}_2} \simeq \frac{4\pi R_{\text{Mars}}^2}{g_{\text{Mars}}} p_{\text{N}_2} \approx 1.9 \times 10^{18} \text{ kg}, \quad (5)$$

comparable to the mass of a 0.5 bar planetary atmosphere.

1. External sourcing.

If buffer gas must be imported (as N₂, NH₃, or N-bearing ices), the dominant physical cost is momentum. A crude lower bound on the energy to deliver mass M with characteristic hyperbolic excess Δv is the kinetic energy

$$E_k \gtrsim \frac{1}{2} M \Delta v^2. \quad (6)$$

For $M \sim 10^{18} \text{ kg}$ and $\Delta v \sim 5 \text{ km s}^{-1}$, $E_k \sim 10^{25} \text{ J}$, comparable to the oxygenation energy scale in Eq. (43). In practice, gravitational assists and aerocapture can reduce propulsive energy, but not the fundamental momentum exchange requirement.

Eq. (6) is a kinetic-energy *floor*; in practice, gravity assists and aerocapture can reduce propulsive energy expenditure. However, they do not remove the underlying momentum exchange and mass-handling requirement: capturing, processing, and distributing $\sim 10^{18} \text{ kg}$ of volatiles is primarily a *mass logistics and industrial throughput* problem (navigation/capture, fragmentation control, thermal processing, and global atmospheric delivery), not merely a Δv budgeting exercise.

2. NH₃ as an N-carrier.

If nitrogen is imported primarily as ammonia, photolysis and chemistry can convert it into N₂ while hydrogen escapes, leaving N₂ as a buffer gas. Stoichiometrically, producing one mole of N₂ (28 g) requires two moles of NH₃ (34 g) to supply two N atoms, so the imported mass is at least $\sim 1.21 \times$ the desired N₂ mass, before losses.

These mass and momentum scales imply that E4 atmospheres are difficult to reach without either enormous exogenous mass logistics or a yet-unquantified endogenous nitrogen inventory.

E. How much fixed nitrogen would Mars need to supply a buffer gas?

If Mars were to supply buffer gas endogenously, the limiting question is the global inventory of fixed nitrogen (e.g., nitrates) accessible to mining and release. Let an accessible regolith layer of depth d and bulk density ρ contain a mean nitrogen mass fraction w_N . The total nitrogen mass is

$$M_N \simeq 4\pi R_{\text{Mars}}^2 \rho d w_N, \quad (7)$$

and because N_2 is nitrogen by mass, the achievable buffer-gas pressure is

$$p_{N_2} \simeq \frac{g_{\text{Mars}} M_N}{4\pi R_{\text{Mars}}^2} \simeq g_{\text{Mars}} \rho d w_N. \quad (8)$$

Solving for the required nitrogen mass fraction,

$$w_N \simeq \frac{p_{N_2}}{g_{\text{Mars}} \rho d} \approx 6.7 \times 10^{-2} \left(\frac{p_{N_2}}{50 \text{ kPa}} \right) \left(\frac{\rho}{2000 \text{ kg m}^{-3}} \right)^{-1} \left(\frac{d}{100 \text{ m}} \right)^{-1}. \quad (9)$$

Thus, supplying $p_{N_2} = 50$ kPa from the top ~ 100 m would require an implausibly high planet-wide mean nitrogen fraction (percent-level by mass). Even $d = 1$ km requires $w_N \sim 6.7 \times 10^{-3}$, still extremely large on a global average. This does not rule out regional nitrogen extraction, but it strongly suggests that E4 buffer-gas inventories are more naturally met by exogenous sourcing unless deep, nitrogen-rich deposits exist. In situ observations do indicate fixed nitrogen (nitrate) in Martian sediments, but the global inventory remains poorly constrained [10].

Eq. (8) demonstrates that supplying $\mathcal{O}(10\text{--}50)$ kPa of buffer gas as a *global mean* from shallow regolith requires implausibly large planet-wide w_N . This does not exclude the possibility that *localized* nitrogen-rich deposits could support *regional* E2/E3 domes or paraterraforming zones, because required mass scales with covered area rather than planetary surface area. For a region of area A_{reg} , the buffer-gas mass required to achieve p_{N_2} over that region is

$$M_{N_2, \text{reg}} \simeq \frac{A_{\text{reg}}}{g_{\text{Mars}}} p_{N_2} \simeq 1.35 \times 10^{16} \text{ kg} \left(\frac{A_{\text{reg}}}{10^6 \text{ km}^2} \right) \left(\frac{p_{N_2}}{50 \text{ kPa}} \right), \quad (10)$$

which is $\sim 140\times$ smaller than the global requirement for the same p_{N_2} .

As we have seen, Section III showed that E3 and above are intrinsically exaton-class mass problems: even $P_s = 6.27$ kPa implies $M_{\text{atm}} \approx 2.4 \times 10^{17}$ kg (Table III), and E4 buffer+oxygen inventories exceed 10^{18} kg. However, pressure alone does not imply habitability; the next question is whether Mars can be warmed to $T_s \gtrsim 250\text{--}273$ K under current insolation. Section IV therefore derives radiative targets in the two natural control variables: ΔF_{TOA} for insolation changes and τ_{IR} for greenhouse pathways.

IV. THERMAL REQUIREMENTS: RADIATIVE FORCING AND THE ~ 60 K PROBLEM

A. Global mean forcing needed for large temperature changes

A minimal, transparent way to relate temperature targets to energy balance is through the effective radiating temperature T_e at TOA:

$$\sigma_{\text{SB}} T_e^4 = \frac{S_{\text{Mars}}}{4} (1 - A_B) + \Delta F_{\text{TOA}}, \quad (11)$$

where ΔF_{TOA} is an imposed perturbation to the net absorbed flux (e.g., from orbital mirrors or albedo change). In this simple model, raising T_e from T_{e0} to T_e requires

$$\Delta F_{\text{TOA}} = \sigma_{\text{SB}} (T_e^4 - T_{e0}^4). \quad (12)$$

For Mars, increasing T_e by 30 K (from 210 K to 240 K) requires $\Delta F_{\text{TOA}} \approx 78 \text{ W m}^{-2}$, while 60 K requires $\Delta F_{\text{TOA}} \approx 191 \text{ W m}^{-2}$. These are extremely large global perturbations.

1. Surface temperature T_s vs. T_e : why the same “60 K” implies different requirements.

Eqs. (11)–(12) quantify the top-of-atmosphere (TOA) forcing required to raise the effective radiating temperature T_e directly (e.g., via mirrors or albedo changes). This is the correct metric for *insolation-modifying* approaches. However, greenhouse approaches primarily seek to raise the surface temperature T_s at approximately fixed absorbed solar power by increasing longwave optical depth, thereby increasing T_s relative to T_e . Accordingly, the ΔF_{TOA} values computed above should be interpreted as bounds for *direct TOA forcing* methods, whereas greenhouse methods are more naturally expressed in terms of the required infrared optical depth τ_{IR} (Sec. IV B).

2. Why “waste heat” is not a global terraforming lever.

A useful sanity check is to compare industrial waste heat to planetary radiative fluxes. A global mean forcing of just $\Delta F = 10 \text{ W m}^{-2}$ corresponds to total power $\Delta P = 4\pi R_{\text{Mars}}^2 \Delta F \approx 1.4 \times 10^{15} \text{ W}$, i.e. $\sim 1400 \text{ TW}$. Therefore, even a civilization dissipating $\sim 10 \text{ TW}$ of waste heat would supply only $\sim 0.07 \text{ W m}^{-2}$ globally. Direct heat injection can matter locally, but *global* warming requires radiative (albedo/insolation) or greenhouse modifications.

The surface temperature exceeds T_e when the atmosphere provides greenhouse effect. Terraforming proposals therefore focus on increasing greenhouse opacity (longwave trapping) rather than directly increasing absorbed solar flux. However, any proposed mechanism must ultimately supply an *effective* TOA forcing of comparable scale when expressed in energy-balance terms.

B. Relating TOA forcing to surface temperature: a minimal greenhouse mapping

Terraforming objectives are typically stated in terms of surface temperature T_s , whereas Eqs. (11)–(15) constrain the effective radiating temperature T_e at TOA. Greenhouse interventions primarily alter the mapping $T_s(T_e)$ by increasing longwave optical depth, rather than by imposing a direct TOA forcing ΔF_{TOA} .

A standard first-order approximation is the Eddington grey-atmosphere relation for radiative equilibrium:

$$T_s^4 \simeq \frac{3}{4} T_e^4 \left(\tau_{\text{IR}} + \frac{2}{3} \right), \quad (13)$$

where τ_{IR} is the broadband infrared optical depth from the surface to space. Solving Eq. (13) for the optical depth required to reach a target T_s gives

$$\tau_{\text{IR}} \simeq \frac{4}{3} \left(\frac{T_s}{T_e} \right)^4 - \frac{2}{3}. \quad (14)$$

Note that the grey-atmosphere relation in Eq. (13) is used here only to define an *engineering target* for the order-of-magnitude longwave opacity required to raise T_s at fixed absorbed solar power; it is *not* a substitute for line-by-line radiative transfer or 3-D GCM predictions of a specific Mars climate state.

For Mars’ present $T_{e0} \approx 210 \text{ K}$ (Table II), achieving $T_s = 273 \text{ K}$ implies $\tau_{\text{IR}} \approx 3.1$, while $T_s = 250 \text{ K}$ implies $\tau_{\text{IR}} \approx 2.0$. These values provide a transparent target for greenhouse strategies: CO_2 alone at $P_s \sim \mathcal{O}(10 \text{ mbar})$ does not supply sufficient τ_{IR} under current insolation, consistent with detailed inventory and climate constraints [4].

A further useful mapping relates τ_{IR} to pressure through a mass absorption coefficient κ_{IR} :

$$\tau_{\text{IR}} \sim \kappa_{\text{IR}} \frac{P_s}{g_{\text{Mars}}}, \quad (15)$$

highlighting the trade between (i) increasing P_s (at large gas mass cost) and (ii) increasing κ_{IR} via trace super-greenhouse gases or aerosol absorption in spectral window regions. Eq. (15) is not intended as a substitute for line-by-line radiative transfer, but as a first-order engineering scaling relation that exposes which proposals require exaton-class pressure increases versus those that require high- κ_{IR} engineered constituents.

Uncertainties in translating a target T_s into a required $\tau_{\text{IR,eff}}$ are generically $\mathcal{O}(\pm 30\text{--}50\%)$, driven by non-grey spectral structure (windows vs. saturated bands), dust/cloud feedbacks, lapse-rate changes, and orbital/seasonal variability. This uncertainty does *not* affect the exaton-scale mass conclusions for E3/E4, which follow directly from hydrostatic pressure–mass relation (Sec. III) and composition requirements (Sec. VII).

1. Spectral interpretation of the grey τ_{IR} .

In a non-grey Mars atmosphere, incremental surface warming is often controlled by (i) *spectral window regions* that are weakly absorbing in the baseline state, (ii) *pressure broadening* that extends absorption into line wings, and (iii) cloud/dust feedbacks that redistribute LW opacity and SW heating. Accordingly, the grey τ_{IR} in Eq. (13) should be interpreted as an *effective, window-weighted longwave optical depth* required to obtain a target T_s/T_e , not as a literal spectrally uniform opacity.

For architecture trades it is therefore useful to introduce a “window-filling efficacy” factor $w_{\text{win}} \in (0, 1]$ such that a mechanism with mass absorption coefficient κ_{IR} produces

$$\tau_{\text{IR,eff}} \sim w_{\text{win}} \kappa_{\text{IR}} \frac{P_s}{g_{\text{Mars}}}, \quad (16)$$

where $w_{\text{win}} \sim 1$ for constituents that add opacity primarily in LW window regions and $w_{\text{win}} \ll 1$ for constituents that add opacity mainly in already-saturated bands. Eq. (16) makes explicit that the relevant engineering question is not “how much τ_{IR} is added,” but “how much *window-weighted* opacity can be added per kg m^{-2} column.”

2. Sensitivity to orbital/seasonal radiative state.

The required optical depth depends on T_e through Eq. (14). Using $T_e = [S(1 - A_B)/(4\sigma_{\text{SB}})]^{1/4}$, Mars’ orbit-averaged value is $T_{e0} \approx 210$ K (Table II), but T_e varies with heliocentric distance and albedo. For illustration, if T_e spans ~ 201 – 221 K across Mars’ orbit for fixed $A_B = 0.25$, then the required τ_{IR} for $T_s = 273$ K spans

$$\tau_{\text{IR}}(273 \text{ K}) \approx 2.5\text{--}3.9, \quad (17)$$

compared to $\tau_{\text{IR}} \approx 3.1$ at $T_e = 210$ K. This sensitivity underscores that greenhouse mapping should be treated as a range rather than a point estimate when translating to constituent inventories or aerosol column masses.

C. Why the water triple point is not a sufficient criterion

Exceeding the triple point of water does not ensure stable surface liquid water. Even at $P_s \gtrsim 6.1$ mbar, liquid water can remain metastable only briefly because:

1. *Evaporation into an unsaturated atmosphere.* Mars’ atmosphere is extremely dry; evaporation rates can be high even when boiling is suppressed.
2. *Radiative cooling and freezing.* Without sustained warming, transient melt refreezes quickly.
3. *Local energy balance dominates.* Insolation varies strongly with latitude, season, time of day, and dust loading; liquid water stability is therefore spatially and temporally localized.

The CO_2 inventory study [4] makes this explicit: even if polar CO_2 is mobilized to exceed the triple point, liquid water would not be stable at the surface because the temperature shortfall remains $\mathcal{O}(60 \text{ K})$ and evaporation is rapid.

D. Model validity and uncertainty: what the simplified scalings do and do not claim

The constraints used here are intended as feasibility discriminators, not detailed climate predictions. The grey-atmosphere mapping from T_e to T_s [Eq. (13)] compresses spectral structure (window regions, line saturation, pressure broadening) and dynamical feedbacks (dust, clouds, lapse-rate changes) into a single effective τ_{IR} . Consequently, inferred τ_{IR} targets should be interpreted as order-of-unity ranges (e.g., $\tau_{\text{IR}} \sim 2\text{--}4$ for $T_s \sim 250\text{--}273$ K at present T_e), not point values. Mechanism feasibility is therefore assessed by whether a proposal can plausibly supply $\mathcal{O}(1)$ optical-depth changes (or $\mathcal{O}(10^2) \text{ W m}^{-2}$ TOA forcing for mirror/albedo approaches) at the required timescale and maintenance burden.

Where the scaling indicates feasibility, higher-fidelity coupled 3-D GCM + aerosol microphysics + photochemistry is required to determine stability, spatial structure, and control authority. Where the scaling indicates severe shortfall (e.g., endogenous CO_2 inventories vs. E3/E4 pressures), additional modeling cannot remove the mass deficit.

E. Synthesis: the feasibility rubric implied by the governing constraints

Sections III–IV reduce terraforming to a small set of quantitative targets. For any endpoint E_i (Sec. II A), a proposal must simultaneously satisfy:

1. *Mass inventory constraint*: achieve the required pressure and composition inventories. For E3 ($P_s = 6.27$ kPa), Eq. (1) implies $M_{\text{atm}} \approx 2.4 \times 10^{17}$ kg (Table III). For E4, $p_{O_2} = 21$ kPa implies $M_{O_2} \approx 8.2 \times 10^{17}$ kg [Eq. (41)], and a modest $p_{N_2} = 50$ kPa buffer implies $M_{N_2} \approx 1.9 \times 10^{18}$ kg [Eq. (5)].
2. *Radiative requirement*: provide either (a) direct TOA forcing ΔF_{TOA} (mirrors/albedo) or (b) sufficient longwave optical depth τ_{IR} to raise T_s at fixed absorbed solar power. At current insolation, Eq. (14) implies $\tau_{\text{IR}} \sim 2\text{--}4$ for $T_s \sim 250\text{--}273$ K.
3. *Industrial throughput/power constraint*: supply required inventories/absorbers at rate $\dot{M} = M/t_{\text{build}}$ [Eq. (49)] and power $P = E/t_{\text{build}}$ [Eq. (50)]. Even the reversible minimum for oxygenation is $E_{\text{min}} \approx 1.2 \times 10^{25}$ J [Eq. (43)], corresponding to ~ 380 TW averaged over 10^3 yr.
4. *Stability/maintenance constraint*: ensure the engineered state is stable against loss and sinks. For H_2 -based warming, diffusion-limited escape implies a continuous replenishment requirement [Eqs. (46)–(48); Table VI]. For CO_2 -centric pathways, collapse/condensation introduces hysteresis risk (Sec. VIII D).

This rubric turns the mechanism survey (Secs. V–VI) into a controlled comparison: each mechanism is evaluated by *which constraint dominates* (inventory-limited, radiatively-limited, throughput/power-limited, or maintenance-limited) and whether that dominance shifts with the target endpoint.

We have seen that Section IV provided the radiative yardstick: global melt-class climates require either very large direct forcing ($\Delta F_{\text{TOA}} \sim 10^2$ W m $^{-2}$ for large T_e shifts) or a greenhouse optical depth $\tau_{\text{IR}} \sim 2\text{--}4$ at current absorbed solar power. The remainder of the paper evaluates candidate mechanisms by whether they can plausibly deliver these targets given the mass constraints of Sec. III and the industrial constraints developed later in Sec. IX. We begin with what Mars can supply endogenously (Sec. V).

V. ENDOGENOUS VOLATILE MOBILIZATION: WHAT MARS CAN PROVIDE

A. CO_2 reservoirs and the ~ 20 mbar ceiling

The most cited quantitative constraint on Mars terraforming is the inventory of accessible CO_2 . Using spacecraft observations, [4] estimates that readily accessible reservoirs (polar deposits, adsorbed regolith CO_2 , and near-surface carbonates) plausibly sum to ~ 0.02 bar (20 mbar) of mobilizable CO_2 (their “total mobilizable CO_2 ”), with much larger amounts requiring extreme and observationally disfavored assumptions about deep carbonates and clathrates.

Two consequences follow:

1. *Pressure ceiling*. $P_s \sim 20$ mbar corresponds to $M_{\text{atm}} \sim 7.8 \times 10^{16}$ kg (Table III), far below E3/E4 pressure targets.
2. *Warming ceiling*. For a 20 mbar CO_2 atmosphere, climate models predict warming *less than* 10 K at current solar output [4]. Reaching temperatures close to melting would require ~ 1 bar CO_2 , well beyond mobilizable inventories [4].

a. Implied grey κ_{IR} scale for CO_2 under present insolation. Eq. (15) provides a useful inverse inference. If detailed studies indicate that approaching melting under present solar output would require $p_{CO_2} \sim \mathcal{O}(1)$ bar (as discussed in [4]), then achieving a representative $\tau_{\text{IR}} \sim 3$ at $P_s \sim 10^5$ Pa implies an effective grey

$$\kappa_{\text{IR,eff}} \sim \frac{\tau_{\text{IR}} g_{\text{Mars}}}{P_s} \sim 1 \times 10^{-4} \text{ m}^2 \text{ kg}^{-1}. \quad (18)$$

With this $\kappa_{\text{IR,eff}}$, a $P_s = 20$ mbar CO_2 atmosphere corresponds to $\tau_{\text{IR}} \sim 0.05$, consistent with the conclusion that mobilizable CO_2 inventories cannot provide near-melting global climates.

TABLE V. Mechanism comparison matrix (order-of-magnitude). “One-shot” indicates a fill/build operation dominated by initial deployment, whereas “maintenance” indicates a sustained industrial rate set by loss/removal timescales. Values indicate which constraint dominates: inventory-limited (I), radiatively-limited (R), throughput/power-limited (T), or maintenance-limited (M).

Mechanism	Control variable / efficacy	Required scale (illustrative)	Lifetime / replenishment	Dominant bottleneck / limiting constraint
Endogenous CO ₂ mobilization	P_s increase via released CO ₂ , modest greenhouse	$P_s \lesssim \mathcal{O}(20 \text{ mbar})$	One-shot (mostly), but collapse risk	Inventory ceiling; limited warming [4]; I + R
PFC-class super-GHG	Strong window absorption; κ_{IR} in window bands	Feedstock + synthesis at extreme scale	Long-lived but chemistry-dependent; maintenance	Industrial chemistry/ feedstock; lifetime [12, 13]; T (+M if short-lived)
CO ₂ -H ₂ CIA	Requires f_{H_2} at percent level (model-dependent); p_{H_2} mixing ratio	Requires sustained H ₂ production	Diffusion-limited escape \Rightarrow continuous \dot{M}_{H_2} ; maintenance	H ₂ escape (continuous replenishment) [14]; M + T
Engineered aerosols/nanoparticles	Shortwave absorption per column mass Σ_p ; optical properties	Σ_p at mg m^{-2} class maintained column	Residence time days-month; maintenance	Residence time and injection logistics [6]; M + T
Orbital mirrors	Direct ΔF_{TOA}	A_m continent-scale for global forcing	Maintenance (station-keeping / degradation)	Structure mass + deployment + pointing (global); R + T
Regional aerogel paraterraforming	Local radiative transfer	cm-scale layers over km^2 -continent regions	One-shot (regional) + maintenance of coverage	Manufacturing/placement at area; local operations [5]; T (area/logistics)

B. Energetics of CO₂ release: sublimation versus mining

Releasing polar CO₂ ice is energetically straightforward in principle (sublimation), but not necessarily easy in practice. If the buried south polar CO₂ deposit corresponds to $\sim 0.006 \text{ bar}$ (6 mbar) [4], its mass is $M \approx 2.3 \times 10^{16} \text{ kg}$. Using a representative CO₂ latent heat of sublimation $L_{\text{sub}} \sim 6 \times 10^5 \text{ J kg}^{-1}$ [11], the ideal energy to sublimate this reservoir is $\sim 10^{22} \text{ J}$, or several TW sustained over a century. Mining carbonates is harder: carbonates require heating to $\sim 300^\circ\text{C}$ to release CO₂ [4], implying planet-scale material handling and heat delivery.

The endogenous CO₂ ceiling ($\sim 20 \text{ mbar}$) implies both a pressure shortfall relative to E3/E4 and a warming shortfall relative to melt-class climates. Therefore, any global strategy must rely on engineered opacity/absorbers (PFCs, aerosols, CIA) and/or direct insolation modification (mirrors/albedo), which are treated in Sec. VI.

VI. EXOGENOUS AND ENGINEERED WARMING MECHANISMS

Given the endogenous CO₂ ceiling (Sec. V), any pathway toward $T_s \gtrsim 250 \text{ K}$ or toward E3/E4 endpoints must rely on engineered radiative levers and/or imported volatiles. Table V summarizes the mechanism classes considered here and identifies whether each is primarily a one-shot fill or a sustained maintenance load.

A. Synthetic super-greenhouse gases (PFC-class)

Artificial greenhouse gases (perfluorocarbons and related species) have been proposed to warm Mars efficiently because of strong absorption in infrared window regions and long chemical lifetimes. Quantitative radiative-convective modeling has been performed for this class of gases [12, 13]. Two engineering constraints dominate:

1. *Feedstock and synthesis scale.* Even optimistic assessments imply fluorine availability and industrial throughput far beyond near-term capability. For context, recent analysis of alternative proposals notes that PFC-based warming may require volatilizing $\sim 10^5$ megatons of fluorine [6], i.e. $\sim 10^{14} \text{ kg}$ of feedstock element.
2. *Photochemistry and loss.* Some candidate gases are long-lived, but lifetimes depend on UV flux, atmospheric composition, and catalytic cycles; therefore the required production rate is set by *replacement* in addition to initial fill.

Because PFC warming does not directly provide buffer gas, it must be coupled to a separate pressure-building pathway to achieve E3/E4.

B. CO₂–H₂ collision-induced absorption

CO₂–H₂ collision-induced absorption (CIA) can provide substantial greenhouse warming at low pressures. This mechanism has been invoked for early Mars [14]. For terraforming, CIA is attractive because H₂ is lightweight (high molar greenhouse potency per unit mass) and can be produced *in situ* from water via electrolysis, with O₂ as a co-product. However, hydrogen escapes efficiently from Mars, so any H₂-based warming requires sustained replenishment. A complete system analysis therefore couples:

$$\text{required } p_{\text{H}_2} \iff \text{required production rate } \dot{M}_{\text{H}_2} \iff \text{power } P. \quad (19)$$

Even if CIA can warm Mars significantly at sub-bar pressures, it is best viewed as a *maintenance* load rather than a one-time fill.

1. Bracketed mapping: CIA warming implies a required f_{H_2} and (potentially) a maintenance load

CO₂–H₂ collision-induced absorption (CIA) scales with the frequency of CO₂–H₂ collisions and therefore requires both (i) a sufficiently dense background atmosphere and (ii) an H₂ mixing ratio f_{H_2} at the percent-to-tens-of-percent level in published early-Mars radiative–convective studies [14]. For architecture-level accounting we treat f_{H_2} as the primary control variable and translate it into a diffusion-limited replenishment requirement:

$$\dot{M}_{\text{H}_2} \approx 1.2 \times 10^5 f_{\text{H}_2} \text{ kg s}^{-1}, \quad (20)$$

which gives $\dot{M}_{\text{H}_2} \sim 6 \times 10^3 \text{ kg s}^{-1}$ for $f_{\text{H}_2} = 0.05$ and $\dot{M}_{\text{H}_2} \sim 1.2 \times 10^4 \text{ kg s}^{-1}$ for $f_{\text{H}_2} = 0.10$. If replenishment is provided by water electrolysis, the reversible minimum work per kg of H₂ is $\sim 1.2 \times 10^8 \text{ J kg}^{-1}$, implying a minimum maintenance power

$$P_{\text{H}_2, \text{min}} \sim (0.7\text{--}1.4) \text{ TW} \quad \text{for } f_{\text{H}_2} \sim 0.05\text{--}0.10, \quad (21)$$

before plant inefficiencies and compression/storage. Thus, any CIA pathway that requires f_{H_2} in the few-to-ten percent range couples directly to TW-class power and multi-10³ kg s^{−1} hydrogen production capability, in addition to the background atmospheric mass inventory constraint required to reach the CIA-effective pressure regime.

2. Closing the loop: CIA warming implies a required p_{H_2} and a replenishment power.

One-dimensional radiative–convective studies for CO₂–H₂ CIA show that tens of kelvin of warming can occur for $f_{\text{H}_2} \sim 0.05\text{--}0.2$ in bar-class CO₂ atmospheres [14]. To translate this into engineering scale, consider a representative engineered total pressure P_{tot} and hydrogen fraction f_{H_2} , so that $p_{\text{H}_2} = f_{\text{H}_2} P_{\text{tot}}$. The corresponding global H₂ inventory is

$$M_{\text{H}_2} \simeq \frac{4\pi R_{\text{Mars}}^2}{g_{\text{Mars}}} p_{\text{H}_2}. \quad (22)$$

For example, $P_{\text{tot}} = 0.5 \text{ bar}$ and $f_{\text{H}_2} = 0.05$ implies $p_{\text{H}_2} = 25 \text{ mbar}$ and $M_{\text{H}_2} \approx 1.0 \times 10^{17} \text{ kg}$ using Eq. (2).

Hydrogen escape then sets the ongoing replenishment requirement. Using the diffusion-limited upper bound [Eq. (47)], $f_{\text{H}_2} = 0.05$ implies $\dot{M}_{\text{H}_2} \sim 6 \times 10^3 \text{ kg s}^{-1}$, corresponding to a reversible electrolysis power floor $P_{\text{H}_2, \text{min}} \sim 0.7 \text{ TW}$ (Table VI), before real inefficiencies and compression. Thus, even if CIA provides high radiative leverage, it implies (i) a substantial H₂ inventory tied directly to the total pressure, and (ii) a persistent TW-class industrial metabolism to maintain f_{H_2} against loss.

C. Engineered shortwave-absorbing nanoparticles

A recently quantified proposal is to introduce engineered dust/nanoparticles that absorb solar radiation efficiently, producing warming with minimal mass addition [6]. A key advantage is that radiative heating is achieved by *shortwave*

absorption rather than requiring large greenhouse gas partial pressures. The cost is continuous injection because particles sediment and are scavenged.

As an illustrative conversion, [6] discuss sustained particle injection of order tens of liters per second. A volumetric injection rate $\dot{V} \sim 30 \text{ L s}^{-1}$ corresponds to $\dot{V} \approx 0.03 \text{ m}^3 \text{ s}^{-1}$. For a representative particle bulk density $\rho \sim 3 \times 10^3 \text{ kg m}^{-3}$,

$$\dot{M}_p \sim \rho \dot{V} \sim 90 \text{ kg s}^{-1} \sim 2.8 \times 10^9 \text{ kg yr}^{-1}, \quad (23)$$

or $\sim 3 \times 10^{10} \text{ kg}$ over a decade. This is *small* compared to atmospheric mass requirements (Sec. III), but large as an industrial mass flow, comparable to terrestrial mining/processing streams. The power required depends on mining, comminution, transport, and lofting energy, which are architecture-specific.

A useful normalization is the global-mean surface-area mass flux implied by Eq. (23):

$$\dot{\Sigma}_p \equiv \frac{\dot{M}_p}{4\pi R_{\text{Mars}}^2} \approx 6.2 \times 10^{-13} \text{ kg m}^{-2} \text{ s}^{-1} \approx 20 \text{ mg m}^{-2} \text{ yr}^{-1}, \quad (24)$$

using $4\pi R_{\text{Mars}}^2 \approx 1.44 \times 10^{14} \text{ m}^2$ (Table II). If the effective residence time is $\tau_p \sim 30\text{--}100$ days, the maintained global-mean column mass is $\Sigma_p \sim \dot{\Sigma}_p \tau_p \sim 1.6\text{--}5.4 \text{ mg m}^{-2}$. This provides a direct bridge between industrial injection rate and the “ mg m^{-2} class” entries in Table V.

1. Lifetime and maintenance

Particle-induced warming is a *maintenance* mechanism. If particles have an atmospheric residence time τ_p set by sedimentation and scavenging, maintaining a global column mass Σ_p requires a source flux $\dot{\Sigma}_p \approx \Sigma_p/\tau_p$. At Mars, dust residence times can range from days (local storms) to months (global events), and engineered particles must be designed to balance (i) optical efficiency, (ii) coagulation resistance, and (iii) acceptable health and environmental impacts. Thus, the required injection rates scale inversely with achievable residence time.

2. From maintained column mass to forcing (parametric mapping)

A minimal bridge from maintained particle column mass Σ_p (kg m^{-2}) to radiative impact is via an effective shortwave mass-extinction coefficient κ_{SW} ($\text{m}^2 \text{ kg}^{-1}$):

$$\tau_{\text{SW}} \sim \kappa_{\text{SW}} \Sigma_p. \quad (25)$$

For optically thin to moderate aerosol layers, an order-of-magnitude forcing scaling can be written as

$$\Delta F_{\text{TOA}} \sim \frac{S_{\text{Mars}}}{4} (1 - A_B) \mathcal{E}(\tau_{\text{SW}}, \omega_0, g), \quad (26)$$

where \mathcal{E} encapsulates the dependence on optical depth, single-scattering albedo ω_0 , and asymmetry parameter g . Eqs. (25)–(26) make explicit that feasibility is governed by (i) achievable κ_{SW} for engineered particles, and (ii) achievable residence time τ_p that sets $\Sigma_p \sim \dot{\Sigma}_p \tau_p$. Detailed forcing estimates therefore require microphysical lifetime modeling and radiative transfer, but the scaling above exposes the two key engineering levers that set industrial requirements.

3. Bracketed mapping: from claimed ΔT_s to forcing and maintained column mass

Shortwave (SW) absorbers can deposit energy aloft, warming the atmosphere while reducing surface insolation; therefore a given increase in absorbed solar power does not guarantee a proportional increase in surface temperature. We parameterize this uncertainty with a *surface-warming efficacy* factor $\epsilon_{\text{surf}} \in (0, 1]$, defined such that the absorbed-shortwave perturbation required to achieve a target ΔT_s scales as $\Delta F_{\text{abs}} \propto 1/\epsilon_{\text{surf}}$. Values $\epsilon_{\text{surf}} \ll 1$ correspond to primarily atmospheric heating (weak surface response), implying larger required maintained aerosol columns and injection rates.

To connect “ ΔT_s warming” claims to industrial requirements, we map a representative global-mean temperature change to an *equivalent* TOA forcing assuming the perturbation acts primarily through additional absorbed solar power:

$$\Delta F_{\text{abs}} \equiv \frac{1}{\epsilon_{\text{surf}}} \sigma_{\text{SB}} \left[(T_{e0} + \Delta T_s)^4 - T_{e0}^4 \right], \quad (27)$$

where $\epsilon_{\text{surf}} \in (0, 1]$ is the surface-warming efficacy defined above and $T_{e0} \simeq 210$ K. For $\Delta T = 10$ K this gives $\Delta F_{\text{eq}} \approx 22.6 \text{ W m}^{-2}$. The corresponding albedo-equivalent change is

$$\Delta A_B \simeq -\frac{4 \Delta F_{\text{abs}}}{S_{\text{Mars}}} = -\frac{4}{\epsilon_{\text{surf}}} \frac{\sigma_{\text{SB}} \left[(T_{e0} + \Delta T_s)^4 - T_{e0}^4 \right]}{S_{\text{Mars}}} \approx -0.15 \left(\frac{\Delta F_{\text{abs}}}{22.6 \text{ W m}^{-2}} \right) \left(\frac{589 \text{ W m}^{-2}}{S_{\text{Mars}}} \right). \quad (28)$$

Relating albedo change to an effective shortwave optical depth via an order-unity radiative efficiency factor $\eta_{\text{SW}} \sim \mathcal{O}(0.1\text{--}0.5)$ (capturing single-scattering albedo, asymmetry, and vertical distribution),

$$|\Delta A_B| \sim \eta_{\text{SW}} \tau_{\text{SW}} \Rightarrow \tau_{\text{SW}} \sim \frac{|\Delta A_B|}{\eta_{\text{SW}}}. \quad (29)$$

Taking $\eta_{\text{SW}} = 0.3$ yields $\tau_{\text{SW}} \sim 0.5$ for the $\Delta T = 10$ K case. If particle extinction is parameterized by a mass extinction coefficient $\kappa_{\text{ext}} \sim 10^4\text{--}10^5 \text{ m}^2 \text{ kg}^{-1}$ (strongly absorbing fine particles), then the maintained column mass is

$$\Sigma_p \sim \frac{\tau_{\text{SW}}}{\kappa_{\text{ext}}} \sim (5 \times 10^{-6}\text{--}5 \times 10^{-5}) \text{ kg m}^{-2} \quad (5\text{--}50 \text{ mg m}^{-2}). \quad (30)$$

For an atmospheric residence time $\tau_p \sim 50$ days, the required global injection rate is

$$\dot{M}_p \sim \frac{4\pi R_{\text{Mars}}^2 \Sigma_p}{\tau_p} \sim 10^2\text{--}10^3 \text{ kg s}^{-1}, \quad (31)$$

consistent with the paper’s “maintenance-limited” classification for aerosol pathways. This bracketed estimate is intentionally conservative and can be updated when a specific particle design and radiative efficacy (ΔT_s per Σ_p) is adopted from detailed microphysics/radiative transfer.

Because $\Delta F_{\text{abs}} \propto 1/\epsilon_{\text{surf}}$, [Eq. (27)], the required SW optical depth and maintained particle column scale as

$$\tau_{\text{SW}}, \Sigma_p, \dot{M}_p \propto \frac{1}{\epsilon_{\text{surf}} \eta_{\text{SW}}}. \quad (32)$$

for fixed optical properties (κ_{ext}) and residence time (τ_p). Thus, if $\epsilon_{\text{surf}} = 0.3$ rather than 1, the required maintained column and injection rate increase by $\sim 3.3\times$. This makes explicit that the dominant uncertainty for SW absorbers is *surface-warming control authority* (vertical heating profile, particle altitude, and feedback response), not only mass flow.

4. Closing the forcing loop: from a claimed ΔT_s to an implied maintained column

For a maintenance-limited aerosol pathway, the relevant climate variable is the *steady-state atmospheric* column mass, not the time-integrated mass injected. If particles have an effective atmospheric residence time τ_p (set by sedimentation, coagulation, and scavenging), then the maintained atmospheric mass is $M_{p,\text{atm}} \simeq \dot{M}_p \tau_p$ and the corresponding global-mean column is

$$\Sigma_p \simeq \frac{M_{p,\text{atm}}}{4\pi R_{\text{Mars}}^2} \simeq \frac{\dot{M}_p \tau_p}{4\pi R_{\text{Mars}}^2}. \quad (33)$$

For the illustrative injection $\dot{V} \simeq 30 \text{ L s}^{-1}$ and $\rho \simeq 3 \times 10^3 \text{ kg m}^{-3}$, Eq. (23) gives $\dot{M}_p \simeq 90 \text{ kg s}^{-1}$ and hence $\dot{\Sigma}_p \simeq 6.2 \times 10^{-13} \text{ kg m}^{-2} \text{ s}^{-1}$. If $\tau_p \sim 30\text{--}100$ days, then $\Sigma_p \sim 1.6\text{--}5.4 \text{ mg m}^{-2}$. Conversely, achieving $\Sigma_p \sim 0.2 \text{ g m}^{-2}$ at the same \dot{M}_p would require $\tau_p \sim 10$ years (or, for $\tau_p \sim 50$ days, $\dot{M}_p \sim 6 \times 10^3 \text{ kg s}^{-1}$). The cumulative injected mass over 10 years is $M_{p,\text{inj}} = \dot{M}_p t$, but only the fraction $\sim \tau_p/t$ contributes to the instantaneous atmospheric loading.

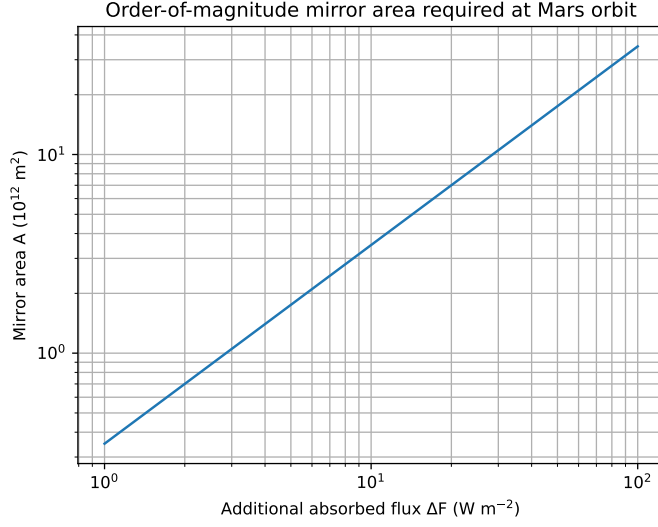


FIG. 2. Order-of-magnitude mirror area required to supply a global mean additional absorbed flux ΔF_{TOA} at Mars orbit, using Eq. (36) with $\eta_m = 0.7$ and $S_{\text{Mars}} = 589 \text{ W m}^{-2}$ [9].

Interpreting $\Delta T_s \sim 30 \text{ K}$ as raising T_s from $\sim 210 \text{ K}$ to $\sim 240 \text{ K}$, the minimal grey-atmosphere approximation [Eq. (14)] implies a required effective longwave optical depth $\tau_{\text{IR}} \approx 1.6$ at $T_e \approx 210 \text{ K}$. If one attributes this warming to an effective radiative opacity proportional to particle column, an order-of-magnitude mass-specific opacity is

$$\kappa_{\text{eff}} \sim \frac{\tau_{\text{IR}}}{\Sigma_p} \sim 8 \times 10^3 \text{ m}^2 \text{ kg}^{-1}, \quad (34)$$

illustrating why aerosols can be mass-efficient compared to gases. Under the same linear-in-column assumption, achieving $T_s \approx 273 \text{ K}$ ($\tau_{\text{IR}} \approx 3.1$) would require $\Sigma_p \sim 0.4 \text{ g m}^{-2}$, i.e. $\sim 2 \times$ the maintained column (and thus $\sim 2 \times$ the sustained injection) for fixed particle lifetime and optical properties.

These mappings are intentionally bracketed estimates: real outcomes depend on vertical heating profiles, microphysics (coagulation/sedimentation), and spectral properties, and therefore require coupled aerosol and radiative-transfer modeling for accuracy.

D. Orbital mirrors and albedo modification

Directly increasing absorbed solar flux is conceptually simple but scale-limited. Suppose one seeks an average TOA forcing ΔF_{TOA} by adding reflected sunlight. The additional absorbed power is

$$\Delta P = 4\pi R_{\text{Mars}}^2 \Delta F_{\text{TOA}}. \quad (35)$$

A mirror of area A_m at Mars orbit intercepts solar power $S_{\text{Mars}} A_m$. If an overall efficiency η_m accounts for reflectivity, pointing, and geometric losses, then

$$A_m \simeq \frac{4\pi R_{\text{Mars}}^2 \Delta F_{\text{TOA}}}{\eta_m S_{\text{Mars}}}. \quad (36)$$

Combining the definition of global mean forcing with intercepted solar flux yields Eq. (36). For a quick estimate, the mirror area scaling is given by

$$A_m \approx 7.0 \times 10^{12} \left(\frac{\Delta F_{\text{TOA}}}{20 \text{ W m}^{-2}} \right) \left(\frac{0.7}{\eta_m} \right) \left(\frac{589 \text{ W m}^{-2}}{S_{\text{Mars}}} \right) \text{ m}^2. \quad (37)$$

Figure 2 shows this scaling for $\eta_m = 0.7$. Even a modest global forcing $\Delta F_{\text{TOA}} = 20 \text{ W m}^{-2}$ implies $A_m \sim 7 \times 10^{12} \text{ m}^2$ ($\sim 7 \times 10^6 \text{ km}^2$), a continent-scale structure.

Albedo reduction is a related lever. Because absorbed solar is $S_{\text{Mars}}(1 - A_{\text{B}})/4$, a change ΔA_{B} yields

$$\Delta F_{\text{TOA}} \approx -\frac{S_{\text{Mars}}}{4} \Delta A_{\text{B}}. \quad (38)$$

Reducing A_{B} by 0.05 provides only $\sim 7 \text{ W m}^{-2}$, illustrating that large temperature changes require either very large albedo changes, very large mirrors, or strong greenhouse feedbacks.

1. Mirror mass scaling

Mirror area is not the only constraint: total mirror mass scales as

$$M_m \sim \sigma_m A_m, \quad (39)$$

where σ_m is areal density. For $A_m \sim 7 \times 10^{12} \text{ m}^2$ (Fig. 2) and $\sigma_m \sim 1\text{--}10 \text{ g m}^{-2}$, the mirror mass is $M_m \sim 10^{10}\text{--}10^{11} \text{ kg}$, comparable to a large terrestrial megaproject and likely requiring in-space manufacturing for credibility.

2. Mirror scale for melt-class forcing

The $\sim 60 \text{ K}$ ‘‘melt-class’’ deficit corresponds to $\Delta F_{\text{TOA}} \approx 191 \text{ W m}^{-2}$ for a direct T_e increase from 210 K to 270 K [Eq. (12)]. Using Eq. (36), this implies a mirror area larger by a factor $\sim 191/20 \approx 9.6$ than the $\Delta F_{\text{TOA}} = 20 \text{ W m}^{-2}$ example, i.e. $A_m \sim 7 \times 10^{13} \text{ m}^2 \sim 7 \times 10^7 \text{ km}^2$, before additional geometric and control losses. This highlights why mirrors are best viewed as a high-authority but extreme-structure lever.

As we have seen, Section VI had shown that substantial warming can, in principle, be achieved with relatively small added atmospheric mass, but typically at the cost of sustained maintenance (H_2 replenishment, aerosol injection) or extreme structures (mirrors). Importantly, warming alone does not deliver a breathable atmosphere: E4 is dominated by O_2 and buffer-gas inventories and their associated energy and throughput requirements. Section VII quantifies these composition-driven requirements.

VII. OXYGENATION AND BREATHABLE ENDPOINTS

A. O_2 mass required for breathable partial pressures

A breathable atmosphere requires substantial O_2 partial pressure. Using Eq. (1), the mass of O_2 corresponding to a partial pressure p_{O_2} is

$$M_{\text{O}_2} \simeq \frac{4\pi R_{\text{Mars}}^2}{g_{\text{Mars}}} p_{\text{O}_2}. \quad (40)$$

For $p_{\text{O}_2} = 21 \text{ kPa}$ (Earth-like),

$$M_{\text{O}_2} \approx 8.2 \times 10^{17} \text{ kg}. \quad (41)$$

This is already comparable to the total mass of a 0.2 bar atmosphere.

B. Thermodynamic minimum energy to produce O_2 from water

Producing O_2 by electrolyzing water,



requires a minimum Gibbs free energy input ΔG° per mole of O_2 . Using standard thermochemical data [15], the reversible minimum at 298 K is $\Delta G^\circ \approx 474 \text{ kJ mol}^{-1}$ per mole of O_2 ($\approx 14.8 \text{ MJ kg}^{-1}$ of O_2). Therefore, the idealized minimum energy to produce Eq. (41) is

$$E_{\text{min}} \approx \left(\frac{M_{\text{O}_2}}{0.032 \text{ kg mol}^{-1}} \right) \Delta G^\circ \approx 1.2 \times 10^{25} \text{ J}. \quad (43)$$

Real systems require larger energy due to overpotentials, compression/liquefaction, plant losses, and ancillary mining/processing. Even the theoretical minimum corresponds to an average power of ~ 380 TW sustained for 1000 yr, illustrating that E4 endpoints are *energy-dominated*.

Stoichiometrically, producing one kilogram of O_2 from water requires $36/32 = 1.125$ kg of H_2O processed. Thus producing $M_{O_2} \approx 8.2 \times 10^{17}$ kg implies processing $M_{H_2O} \approx 9.2 \times 10^{17}$ kg of water, equivalent to a global water layer of thickness $\sim M_{H_2O}/(\rho_w 4\pi R_{\text{Mars}}^2) \approx 6$ m for $\rho_w \approx 1000$ kg m $^{-3}$.

C. MOXIE as a scale anchor

MOXIE demonstrated oxygen production from atmospheric CO_2 on Mars [16, 17]. Such demonstrations are crucial technology anchors, but scaling to terraforming quantities is extreme. A breathable-atmosphere inventory $M_{O_2} \sim 10^{18}$ kg is $\sim 10^{19}$ times larger than an $\mathcal{O}(10^2)$ g-class technology demonstration output, even before accounting for compression, storage, distribution, and O_2 sinks into the regolith and crust. Therefore oxygenation is not a “scale-up by a factor of ten” problem; it is an orders-of-magnitude industrial civilization problem.

D. O_2 sinks: oxidation capacity of a basaltic regolith/crust can be comparable to atmospheric targets

A breathable endpoint requires not only producing M_{O_2} (Sec. VII), but also overcoming sinks as O_2 oxidizes reduced minerals. A simple bound is obtained by assuming an accessible oxidizable layer of thickness d and density ρ with a representative FeO mass fraction w_{FeO} characteristic of basaltic materials on Mars (e.g., FeO ~ 18 wt% in Mars-relevant silicates [18, 19]).

If FeO is oxidized to Fe_2O_3 via $4FeO + O_2 \rightarrow 2Fe_2O_3$, the required moles of O_2 per mole of FeO is $1/4$. The corresponding O_2 mass sink capacity of a global layer is approximately

$$M_{O_2, \text{sink}}(t) \sim \frac{1}{4} \left(\frac{w_{\text{FeO}} 4\pi R_{\text{Mars}}^2 \rho d_{\text{eff}}(t)}{\mu_{\text{FeO}}} \right) \mu_{O_2}, \quad (44)$$

where μ_{FeO} and μ_{O_2} are molar masses. Numerically,

$$M_{O_2, \text{sink}}(t) \sim 9 \times 10^{17} \text{ kg} \left(\frac{w_{\text{FeO}}}{0.18} \right) \left(\frac{\rho}{3000 \text{ kg m}^{-3}} \right) \left(\frac{d_{\text{eff}}(t)}{100 \text{ m}} \right), \quad (45)$$

comparable to the atmospheric inventory required for $p_{O_2} \sim 21$ kPa (Sec. VII). This illustrates that oxygenation is generically a coupled production-plus-sink-filling problem, and that the energy and timescales in Sec. VII should be interpreted as optimistic lower bounds.

The relevant sink capacity is set by an *effective oxidizable depth* $d_{\text{eff}}(t)$, not necessarily the full geometric depth of regolith/crust, because oxygen uptake depends on kinetics, permeability, and how much fresh reduced material is exposed by impacts, dust gardening, and (critically) human excavation and construction. In a systems sense, oxygenation couples to an intentional strategy for managing $d_{\text{eff}}(t)$: *passivation* (oxidize reactive material in engineered reactors), *sealing/vitrification* or surface stabilization to reduce atmospheric access, and *controlled excavation* to avoid continually exposing fresh reduced minerals. Naming $d_{\text{eff}}(t)$ makes explicit that sink-filling is not only a “one scary number” but a coupled design and operations variable in a long-duration terraforming architecture.

As we have seen above, Section VII demonstrates that breathable endpoints are fundamentally energy- and sink-limited: $M_{O_2} \sim 10^{18}$ kg and $E_{\text{min}} \sim 10^{25}$ J even before inefficiencies, and regolith oxidation can absorb an O_2 inventory comparable to atmospheric targets. Whether such inventories persist requires explicit accounting of escape, condensation collapse, and geochemical sequestration, which motivates the stability analysis in Sec. VIII.

VIII. ATMOSPHERIC LOSS, RETENTION, AND CONTROL

A terraformed Mars must retain its engineered atmosphere against escape to space and against surface sequestration (carbonates, adsorption, polar condensation).

A. Escape to space: why it matters more for H_2 than for CO_2

MAVEN observations quantify present-day atmospheric loss and its dependence on solar conditions [20]. For heavy species (CO_2 , N_2), bar-level atmospheres have enormous mass and are likely to be lost on geological timescales

TABLE VI. Illustrative diffusion-limited H₂ replenishment requirements using Eq. (47) and a reversible electrolysis specific energy of 1.2×10^8 J kg⁻¹ of H₂.

f_{H_2}	\dot{M}_{H_2} (kg s ⁻¹)	$P_{H_2,\min}$ (TW)
0.01	1.2×10^3	0.14
0.05	6.0×10^3	0.72
0.10	1.2×10^4	1.44

even without a global magnetic field, whereas for hydrogen the escape timescale can be short (diffusion-limited and hydrodynamic escape). Thus, H₂-based warming (Sec. VIB) implies a persistent production requirement.

B. Artificial magnetic shielding

One proposed mitigation is to reduce solar-wind stripping by placing a magnetic dipole or plasma shield upstream of Mars, such as near Mars–Sun L1, thereby expanding the induced magnetosphere and reducing ion escape [21]. This approach does not create atmosphere by itself; it is a retention and radiation-environment tool. Its engineering feasibility depends on field strength, standoff distance, power, and superconducting/structure mass, which require dedicated systems studies beyond the scope of this first-order paper.

C. Hydrogen escape sets a continuous maintenance throughput for CO₂–H₂ warming

A key distinction between CO₂-mass-based warming and CO₂–H₂ CIA warming is that hydrogen can be lost rapidly, implying a persistent replenishment requirement. A standard upper bound on hydrogen escape is the diffusion-limited flux, often expressed in terms of the hydrogen atom flux (“H equivalents”) (e.g., [22, 23]):

$$\Phi_{\text{DL,H}} \approx \Phi_0 f_H, \quad (46)$$

where f_H is the total hydrogen mixing ratio expressed as H atoms (summing over all H-bearing species). If hydrogen is supplied primarily as H₂, then $f_H \approx 2f_{H_2}$ and the corresponding H₂ molecular flux is $\Phi_{\text{DL,H}_2} \approx \frac{1}{2}\Phi_{\text{DL,H}} \approx \Phi_0 f_{H_2}$. The corresponding global H₂ mass loss rate is then

$$\dot{M}_{H_2} \approx 4\pi R_{\text{Mars}}^2 m_{H_2} \Phi_{\text{DL,H}_2} \approx 1.2 \times 10^5 \left(\frac{\Phi_0}{2.5 \times 10^{13} \text{ cm}^{-2} \text{ s}^{-1}} \right) f_{H_2} \text{ kg s}^{-1}, \quad (47)$$

where m_{H_2} is the molecular mass of H₂ and we used Mars’ surface area for scaling.

Even modest f_{H_2} can therefore imply $\dot{M}_{H_2} \sim 10^3$ – 10^4 kg s⁻¹ class replenishment. If H₂ is produced by water electrolysis, the reversible specific energy is $\sim 1.2 \times 10^8$ J kg⁻¹ of H₂, implying a minimum maintenance power

$$P_{H_2,\min} \sim 0.1\text{--}1 \text{ TW} \quad \text{for} \quad \dot{M}_{H_2} \sim 10^3\text{--}10^4 \text{ kg s}^{-1}, \quad (48)$$

before compression, storage, and plant inefficiencies. Therefore CO₂–H₂ warming is best analyzed as a sustained industrial metabolism rather than a one-shot fill.

D. CO₂ condensation and atmospheric collapse: a stability constraint on CO₂-centric pathways

CO₂-centric terraforming pathways must contend with the possibility of atmospheric collapse, i.e., condensation of CO₂ into permanent polar deposits that reduce P_s and weaken greenhouse warming. Three-dimensional climate simulations of early Mars with 0.1–7 bar CO₂ atmospheres show that CO₂ ice clouds, obliquity, dust loading, and surface properties can lead to climates where CO₂ condensation and cold trapping limit warming and can induce collapse-like behavior under some conditions [24].

In a first-order control sense, CO₂ stability requires maintaining polar temperatures above the CO₂ condensation threshold for the prevailing p_{CO_2} . Thus, even if CO₂ is available in principle, the engineered climate may require active control authority (e.g., directed insolation, albedo management, or supplemental absorbers) to avoid pressure-loss hysteresis and to keep the system on a warm branch.

TABLE VII. Representative energetic scales (order-of-magnitude).

Operation	Scale assumption	Energy / size
Sublimate ~ 6 mbar CO ₂ polar deposit	$M \sim 2.3 \times 10^{16}$ kg, $L_{\text{sub}} \sim 6 \times 10^5$ J/kg	$\sim 1 \times 10^{22}$ J
Produce Earth-like $p_{\text{O}_2} = 21$ kPa from water	$M_{\text{O}_2} \sim 8 \times 10^{17}$ kg, reversible ΔG°	$\sim 1 \times 10^{25}$ J
Global forcing by orbital mirrors	$\Delta F_{\text{TOA}} = 20$ W m ⁻² , $\eta_m = 0.7$	$A_m \sim 7 \times 10^{12}$ m ²
Decadal engineered nanoparticle injection	$\dot{V} = 30$ L s ⁻¹ , $\rho = 3 \times 10^3$ kg m ⁻³	$\sim 3 \times 10^{10}$ kg/decade

TABLE VIII. Illustrative throughput and power requirements for representative endpoints, showing the scaling with assumed build time. Values use $M_{\text{O}_2} \approx 8.2 \times 10^{17}$ kg for $p_{\text{O}_2} = 21$ kPa [Eqs. (40)–(41)], $M_{\text{N}_2} \approx 1.9 \times 10^{18}$ kg for $p_{\text{N}_2} = 50$ kPa [Eq. (5)], and $E_{\text{min}} \approx 1.2 \times 10^{25}$ J for reversible electrolysis [Eq. (43)].

Target	M_{target} (kg)	t_{build}	\dot{M}_{req} (kg s ⁻¹)	P_{avg} (TW)
O ₂ for $p_{\text{O}_2} = 21$ kPa	8.2×10^{17}	10 ³ yr	2.6×10^7	380
O ₂ for $p_{\text{O}_2} = 21$ kPa	8.2×10^{17}	10 ² yr	2.6×10^8	3800
N ₂ buffer for $p_{\text{N}_2} = 50$ kPa	1.9×10^{18}	10 ³ yr	6.0×10^7	—
N ₂ buffer for $p_{\text{N}_2} = 50$ kPa	1.9×10^{18}	10 ² yr	6.0×10^8	—

IX. ENERGY DELIVERY AND SYSTEM ARCHITECTURE

A. Energetic “success” thresholds

Table VII summarizes representative energy scales for several canonical operations. These numbers should be interpreted as *lower bounds*; real architectures add large multiplicative factors for inefficiency, infrastructure, and operations.

B. Throughput requirement: required mass flow and average power versus build time

For any proposed endpoint with target inventory M_{target} achieved over a build time t_{build} , the implied mean industrial throughput is

$$\dot{M}_{\text{req}} \equiv \frac{M_{\text{target}}}{t_{\text{build}}}. \quad (49)$$

Likewise, for an intervention requiring integrated energy E , the implied mean power is

$$P_{\text{avg}} \equiv \frac{E}{t_{\text{build}}}. \quad (50)$$

These relations are decisive because they convert “large but abstract” quantities into concrete kg s⁻¹ and TW requirements that can be compared with industrial analogs and with plausible Mars power architectures.

Table VIII emphasizes that breathable endpoints (E4) are not merely “large”: they imply sustained, multi-decade to multi-millennial industrial mass flow rates orders of magnitude above the maintenance rates implied by aerosol-based warming proposals [6]. This does not prove impossibility, but it places E4 in the category of long-duration planetary industry rather than “scale-up of demonstrated ISRU.”

Equations of the form $\dot{M} \sim M/t_{\text{build}}$ convert a thermodynamic/atmospheric end-state requirement into a required *continuous industrial mass flow*. This is the correct discriminator for feasibility because it folds together mining, chemical processing, plant uptime, logistics, maintenance, and scaling laws for an autonomous industrial base. To make these rates interpretable, Sec. XD benchmarks them against present-day terrestrial energy use and bulk material production.

C. Power generation scaling: solar versus nuclear

Any sustained terraforming activity is power-limited. Using the global mean absorbed solar flux on Mars, $\langle F_{\odot} \rangle = S_{\text{Mars}}(1 - A_{\text{B}})/4 \approx 110$ W m⁻² (Table II), the *global-mean* electrical power density from photovoltaics is at best

TABLE IX. Photovoltaic (PV) area required to supply average electrical power on Mars using Eq. (51) with $S_{\text{Mars}} = 589 \text{ W m}^{-2}$ and $A_B = 0.25$ [9]. Values are global-mean lower bounds; real installations require additional area for latitude, dust, night, and storage.

Average power	A_{pv} at $\eta_{\text{pv}} = 0.2$	A_{pv} at $\eta_{\text{pv}} = 0.3$
1 TW	$4.5 \times 10^4 \text{ km}^2$	$3.0 \times 10^4 \text{ km}^2$
10 TW	$4.5 \times 10^5 \text{ km}^2$	$3.0 \times 10^5 \text{ km}^2$
100 TW	$4.5 \times 10^6 \text{ km}^2$	$3.0 \times 10^6 \text{ km}^2$
1000 TW	$4.5 \times 10^7 \text{ km}^2$	$3.0 \times 10^7 \text{ km}^2$

$\eta_{\text{pv}} \langle F_{\odot} \rangle$, where η_{pv} includes conversion efficiency and system losses. Thus, the panel area required for an average electrical power P is

$$A_{\text{pv}} \approx \frac{P}{\eta_{\text{pv}} S_{\text{Mars}} (1 - A_B) / 4}. \quad (51)$$

For $\eta_{\text{pv}} = 0.2$, this implies $\sim 4.5 \times 10^4 \text{ km}^2$ of panels per TW of average power. Table IX reports representative values.

All mirror and PV areas reported here are optimistic lower bounds; realistic designs increase required area by factors of a few to account for pointing losses, dust, latitude, diurnal cycling, seasonal insolation, and storage. These areas are not physically impossible, but they imply continent-scale deployment and maintenance, plus storage for night and multi-week dust storms. High-capacity fission or fusion provides an alternative with much higher power density but large development and safety overhead. Most plausible long-term architectures are therefore *hybrid*: nuclear baseload plus solar where practical, with large-scale energy storage and distribution.

D. Architecture as a coupled control problem

Terraforming is not a single technology; it is a *planetary-scale control system* with feedbacks and constraints. A credible architecture must include:

1. *Energy generation and transmission.* MW–TW class power implies large-scale fission, fusion, or space-based solar power with high reliability. Energy delivery is limited by transmission (surface grids, microwave/laser beaming, or distributed reactors).
2. *Mass production and logistics.* Gas production (O_2 , H_2), particle manufacture, or volatile import requires gigaton/yr class industrial throughput sustained for centuries for global endpoints.
3. *Climate monitoring and feedback control.* Global albedo and aerosol distributions evolve with storms and seasons. A terraforming program must incorporate continuous sensing (orbiters) and active control authority (factory throttling, mirror pointing, particle injection) to maintain targets.
4. *Planetary protection and biosafety constraints.* While outside the scope of this technical paper, any biological component (photosynthetic oxygenation, microbial soil engineering) introduces risk management constraints and long time constants.

E. Staged roadmap: from regional habitability to global modification

Given the scale barriers for E4 endpoints, a technically plausible progression is:

- *Phase I (decades): regional paraterraforming.* Deploy solid-state greenhouse layers (silica aerogel) over ice-rich terrain to enable persistent melt and photosynthesis locally without global atmospheric change [5].
- *Phase II (century): climate nudging and resource mobilization.* Use localized warming to trigger limited volatile release, deploy pilot aerosol systems, and build power and manufacturing base.
- *Phase III (multi-century): sustained atmospheric engineering.* If pursued, combine a stable warming mechanism (aerosols/PFC/CIA) with buffer gas import or extraction and large-scale oxygen production, while simultaneously investing in retention (magnetic shielding) and geochemical management.

This staged view recognizes that the fastest path to meaningful surface habitability is likely *regional* rather than *planetary*.

X. DISCUSSION AND IMPLICATIONS

The constraint-based framework in Table IV shows that the dominant feasibility constraint shifts sharply with the target end state. For regional endpoints (E1–E2), deployment area and local power dominate; for global pressure (E3), atmospheric inventory dominates; and for breathable endpoints (E4), composition inventories, minimum work, and sink filling dominate. For near-term habitability return per unit industrial scale, the results favor regional approaches: paraterraforming and contained biospheres, local thermal/insulation control, and build-out of power and autonomous manufacturing. If global modification is pursued, credible architectures must be evaluated as coupled control systems that explicitly close (i) inventory sourcing, (ii) radiative authority, (iii) sustained throughput and power, and (iv) retention/sink management over multi-century timescales.

A. Which constraint dominates depends on the endpoint

A central implication of the constraint-based framework is that the limiting factor shifts with the target end state:

- For E1–E2 (regional water stability, protected agriculture), the dominant constraints are local radiative control and deployment area; global exatone-scale gas inventories are not required.
- For E3 (no ebullism), the dominant constraint becomes atmospheric mass: $M_{\text{atm}} \approx 2.4 \times 10^{17}$ kg (Table III), plus enough warming to avoid CO₂ collapse.
- For E4 (breathable), the dominant constraints are composition inventories and energy: $M_{\text{O}_2} \approx 8.2 \times 10^{17}$ kg and $M_{\text{N}_2} \approx 1.9 \times 10^{18}$ kg, with reversible oxygenation energy $E_{\text{min}} \approx 1.2 \times 10^{25}$ J (Sec. VII) and additional sink-filling (Sec. VII D).

Where the scaling suggests feasibility (aerosols/CIA), quantitative climate outcomes still require coupled 3-D GCM + aerosol microphysics for a better than an order-of-magnitude accuracy.

B. Design rules implied by the numbers

The results above imply several robust design rules:

1. *Warming-only proposals cannot shortcut buffer-gas and oxygen inventories.* Even if T_s targets are met via aerosols or CIA, E4 remains dominated by 10^{18} kg-class O₂ and N₂/Ar.
2. *Mass-efficient radiative levers tend to be maintenance-limited.* For nanoparticles, Eq. (23) implies $\dot{M}_p \sim 90$ kg s⁻¹, i.e. $\sim 3 \times 10^9$ kg yr⁻¹, and the maintained column mass scales as $\Sigma \sim \dot{\Sigma} \tau_p$ (Sec. VI C). For CO₂–H₂ CIA, Table VI implies $\mathcal{O}(0.1\text{--}1)$ TW-class minimum maintenance power even for modest f_{H_2} .
3. *One-shot forcing is structure-mass-limited.* Eq. (36) implies continent-scale mirrors for ΔF_{TOA} of order 10–20 W m⁻², with total mass $M_m \sim \sigma_m A_m$ in the $10^{10}\text{--}10^{11}$ kg range for $\sigma_m \sim 1\text{--}10$ g m⁻².
4. *E4 is a planetary industry problem: power + throughput + control.* Even at thermodynamic minima, E_{min} implies ~ 380 TW averaged over 10^3 yr, and Table VIII implies $\dot{M} \sim 10^7\text{--}10^8$ kg s⁻¹ for century-to-millennial build times—far beyond “scaled ISRU.”

C. Technology implications and a credible maturation path

If the objective is to maximize near-term habitability impact per unit industrial scale, the results favor: (i) regional paraterraforming (solid-state greenhouse) and enclosed agriculture; (ii) MW–GW-class power and localized thermal control; and (iii) atmospheric monitoring/control infrastructure. If global endpoints are pursued, the pacing technologies become continent-scale energy generation, multi-gigaton/year materials handling, and long-duration closed-loop climate control (sensing + actuation), not a single “magic gas.”

D. Industrial scaling, timescale–power trade, and cost floors

A central result of this paper is that once the endpoint moves beyond E2–E3, feasibility is governed less by the existence of a mechanism and more by whether an autonomous industrial base can sustain the required *mass flow* and *power* for centuries to millennia. For the nominal E4 targets summarized above, the required atmospheric inventories are $M_{\text{O}_2} \simeq 8.2 \times 10^{17}$ kg and $M_{\text{N}_2} \simeq 1.9 \times 10^{18}$ kg, with a minimum reversible electrochemical work $E_{\text{min}} \simeq 1.2 \times 10^{25}$ J for oxygenation alone (exclusive of compression, losses, and co-products).

1. Dominant constraint as a function of end state

For E1–E2 regional habitability, the dominant constraints are deployment area and local power; global volatile inventories are not required. For E3 global pressure, the mass inventory constraint becomes dominant ($M_{\text{atm}} \sim 2.4 \times 10^{17}$ kg at the Armstrong limit). For E4 breathable endpoints, composition inventories and energy dominate: $M_{\text{O}_2} \sim 8 \times 10^{17}$ kg and buffer gases at the 10^{18} kg scale, with oxygenation work $E_{\text{min}} \sim 10^{25}$ J even at reversible limits.

2. Timescale–power–throughput trade

For any target inventory M achieved over build time t_{build} ,

$$\dot{M} \equiv \frac{M}{t_{\text{build}}}, \quad \bar{P} \equiv \frac{E}{t_{\text{build}}}. \quad (52)$$

These relations translate end states into continuous industrial requirements. For example, $p_{\text{O}_2} = 21$ kPa implies $M_{\text{O}_2} \approx 8.2 \times 10^{17}$ kg, so $\dot{M}_{\text{O}_2} \approx 2.6 \times 10^7$ – 2.6×10^8 kg s^{−1} for $t_{\text{build}} = 10^3$ – 10^2 yr. The reversible oxygenation floor implies $\bar{P}_{\text{min}} \approx 0.38$ – 3.8 PW over the same range. Real systems require $\bar{P} \gtrsim \bar{P}_{\text{min}}/\eta_{\text{sys}}$ with $\eta_{\text{sys}} \ll 1$ once compression, separation, thermal losses, and downtime are included.

3. Benchmarking E4 mass flows against terrestrial industry

For a build time t_{build} , the implied continuous production/import rates are

$$\dot{M}_{\text{O}_2} \simeq \frac{M_{\text{O}_2}}{t_{\text{build}}}, \quad \dot{M}_{\text{N}_2} \simeq \frac{M_{\text{N}_2}}{t_{\text{build}}}. \quad (53)$$

For $t_{\text{build}} = 10^3$ yr this corresponds to $\dot{M}_{\text{O}_2} \approx 8.2 \times 10^{14}$ kg yr^{−1} (≈ 820 Gt yr^{−1}) and $\dot{M}_{\text{N}_2} \approx 1.9 \times 10^{15}$ kg yr^{−1} (≈ 1900 Gt yr^{−1}), i.e. $\mathcal{O}(10^4)$ – $\mathcal{O}(10^5)$ tonnes per second.

As a reality check, global material extraction on Earth has grown from ~ 30 to ~ 106 billion tonnes per year since 1970 [25], and world crude steel production is ~ 1.9 billion tonnes per year [26]. Thus, even under a 10^3 -yr schedule, the *oxygen alone* production rate is of order $\sim 8\times$ present-day total terrestrial material extraction, and $\sim 400\times$ present-day global steel output. The nitrogen buffer requirement is larger still.

Importantly, \dot{M}_{O_2} and \dot{M}_{N_2} are not directly mined “as is”; they must be extracted from feedstocks. If oxygen is produced from mined water ice, the required water throughput is

$$\dot{M}_{\text{H}_2\text{O}} \simeq \frac{36}{32} \dot{M}_{\text{O}_2} \approx 1.125 \dot{M}_{\text{O}_2}. \quad (54)$$

while if oxygen (or nitrogen-bearing species) is extracted from regolith with effective yield f by mass, the required regolith handling is $\dot{M}_{\text{reg}} \sim \dot{M}/f$. For plausible $f \sim 0.01$ – 0.1 , regolith throughput rises by one to two orders of magnitude, pushing the problem decisively into “planetary industry” rather than “chemical plant” scaling.

4. Timescale–power trade: what does “accelerating” E4 actually require?

The minimum average power required to supply the reversible oxygenation work is

$$\bar{P}_{\text{min}} \simeq \frac{E_{\text{min}}}{t_{\text{build}}} \simeq 3.8 \times 10^{14} \text{ W} \left(\frac{10^3 \text{ yr}}{t_{\text{build}}} \right) \left(\frac{E_{\text{min}}}{1.2 \times 10^{25} \text{ J}} \right). \quad (55)$$

TABLE X. Order-of-magnitude comparison between Mars E4 build requirements (for $t_{\text{build}} = 10^3$ yr) and representative present-day terrestrial industry magnitudes.

Quantity	Mars E4 (1000 yr build)	Earth today
\dot{M}_{O_2}	$8.2 \times 10^{14} \text{ kg yr}^{-1} \approx 820 \text{ Gt yr}^{-1}$	—
\dot{M}_{N_2}	$1.9 \times 10^{15} \text{ kg yr}^{-1} \approx 1900 \text{ Gt yr}^{-1}$	—
Global material extraction	—	$\sim 106 \text{ Gt yr}^{-1}$ [25]
World crude steel production	—	$\sim 1.89 \text{ Gt yr}^{-1}$ [26]
Global primary energy (avg)	—	$620 \text{ EJ yr}^{-1} \approx 20 \text{ TW}$ [27]

For $t_{\text{build}} = 10^3$ yr, $\bar{P}_{\text{min}} \approx 380 \text{ TW}$, which is $\sim 19\times$ today’s global primary energy consumption rate ($\approx 620 \text{ EJ yr}^{-1}$) [27]. Conversely, if one demands $t_{\text{build}} \sim 100$ yr, Eq. (55) implies $\bar{P}_{\text{min}} \sim 3.8 \text{ PW}$ *before* accounting for real inefficiencies. Because real systems incur conversion, compression, separation, thermal losses, and downtime, a more realistic requirement is $\bar{P} \sim \bar{P}_{\text{min}}/\eta_{\text{sys}}$ with $\eta_{\text{sys}} \ll 1$, pushing required power further upward.

Using Eq. (51), the PV area required to supply the reversible oxygenation power floor is

$$A_{\text{pv}} \sim (4.5 \times 10^4 \text{ km}^2/\text{TW}) \left(\frac{\bar{P}_{\text{min}}}{1 \text{ TW}} \right) \left(\frac{0.2}{\eta_{\text{pv}}} \right) \frac{1}{C_f}, \quad (56)$$

where $C_f \leq 1$ is an effective capacity factor capturing diurnal cycling, latitude, dust storms, and storage limits. For $\bar{P}_{\text{min}} \approx 380 \text{ TW}$ (1000-yr build), even the optimistic $C_f = 1$ bound implies $A_{\text{pv}} \sim 1.7 \times 10^7 \text{ km}^2$ at $\eta_{\text{pv}} = 0.2$. For $t_{\text{build}} = 100$ yr, $\bar{P}_{\text{min}} \sim 3.8 \text{ PW}$ implies A_{pv} comparable to or exceeding Mars’ total surface area unless power is provided by higher-density sources (nuclear/fusion) or by space-based collection and beaming. This illustrates that accelerating E4 is fundamentally a power-density problem, not only a chemistry problem.

5. Economics: minimal energy-cost floor and capex scaling

Although detailed economics are beyond the scope of this paper, the estimates above imply hard *floors*. The reversible oxygenation energy corresponds to

$$E_{\text{min}} \approx 3.3 \times 10^{18} \text{ kWh}, \quad (57)$$

so even at an optimistic electricity price c_e one has an energy-only floor

$$C_{E,\text{min}} \gtrsim (3.3 \times 10^{18} \text{ kWh}) c_e \approx 1.7 \times 10^{17} \$ \left(\frac{c_e}{0.05 \text{ \$/kWh}} \right), \quad (58)$$

exclusive of capital expenditures, maintenance, and the additional energy required for non-reversible steps (compression, gas separation, transport, and thermal management).

Similarly, if the generation system scales with cost c_W per installed watt, then the capex scaling for sustaining \bar{P} is

$$C_{\text{capex}} \sim c_W \bar{P} \approx 3.8 \times 10^{14} \$ \left(\frac{c_W}{1 \text{ \$/W}} \right) \left(\frac{\bar{P}}{380 \text{ TW}} \right), \quad (59)$$

illustrating that even wildly optimistic c_W values imply civilization-scale investment when \bar{P} is in the multi- 10^{14} W class.

6. What industrial activities are actually implied?

The constraints above map directly onto “industrial primitives” that must exist on Mars (or in cis-Mars space): (i) multi-TW continuous power generation with grid-scale storage resilient to seasonal and dust-storm variability; (ii) bulk excavation and beneficiation at $\gtrsim 10^7$ – 10^9 kg s^{-1} effective throughput (depending on feedstock yield); (iii) chemical processing at the same scale (electrolysis, separations, compression, and long-distance gas handling); (iv) megascale manufacturing and deployment of collectors (PV fields, mirrors, or equivalent) and their maintenance; and (v) long-lived autonomous operations, fault tolerance, and replacement manufacturing. Individual component technologies exist on Earth, but the integration of these primitives into a largely autonomous, self-sustaining industrial ecology on Mars is the dominant feasibility gap for E4. This is why near-term strategies tend to favor E1–E2 (local/regional habitability and paraterraforming), while E3–E4 remain fundamentally long-horizon projects.

E. What would change the feasibility classification?

The conclusions shift only if one (or more) of the following becomes true: (i) discovery of orders-of-magnitude larger accessible CO₂ and/or fixed-nitrogen inventories; (ii) a super-greenhouse constituent with strong window absorption, long lifetime, and abundant in-situ feedstock; (iii) megascale space manufacturing enabling continent-scale mirrors/collectors at low areal mass and manageable station-keeping; (iv) a demonstrated autonomous industrial ecology sustaining multi-TW power and Gt yr⁻¹ class throughput for centuries. Absent such changes, the constraint-based results imply that E1–E2 are near-term plausible, whereas E3–E4 remain planetary-industry, long-horizon projects.

XI. CONCLUSIONS

Terraforming Mars is constrained by coupled planet-scale budgets in atmospheric inventory, radiative forcing/opacity, industrial throughput and power, and long-term stability. Using transparent order-of-magnitude scalings, we find:

1. *Pressure targets are exaton-class.* These targets translate directly into atmospheric mass [Eq. (1)]. E3/E4 endpoints require 10¹⁷–10¹⁸ kg of gas, far above endogenous CO₂ inventories. Hydrostatic balance implies $M_{\text{atm}} \simeq 3.89 \times 10^{15}$ kg per mbar [Eq. (2)]. Thus, even the Armstrong-limit pressure ($P_s = 6.27$ kPa) corresponds to $M_{\text{atm}} \approx 2.4 \times 10^{17}$ kg (Table III).
2. *Endogenous CO₂ is inventory-limited and cannot deliver melt-class global climates.* Mobilizable CO₂ plausibly caps at ~ 20 mbar (Sec. V), yielding $\lesssim 10$ K warming under present insolation, leaving a ~ 60 K melt-class shortfall to globally stable surface liquid water.
3. *Melt-class T_s requires either $\tau_{\text{IR}} \sim 2\text{--}4$ at current insolation or extreme direct forcing.* Thermal targets require very large effective forcing. Accessible CO₂ (~ 20 mbar) yields $\lesssim 10$ K warming, whereas ~ 60 K is needed for globally stable surface liquid water [4]. In a minimal grey-atmosphere approximation, $T_s \sim 250\text{--}273$ K at $T_e \approx 210$ K requires $\tau_{\text{IR}} \sim 2\text{--}4$ (Table IV; Eq. (14), Sec. IV B). Direct insolation modification requires ΔF_{TOA} at the $\mathcal{O}(10^2)$ W m⁻² level for large T_e shifts, implying continent-scale mirrors for $\Delta F_{\text{TOA}} \sim \mathcal{O}(10^2)$ W m⁻² (Eq. (12); Eq. (36)).
4. *Breathable endpoints are composition- and energy-dominated.* Earth-like $p_{\text{O}_2} = 21$ kPa implies $M_{\text{O}_2} \approx 8.2 \times 10^{17}$ kg [Eq. (41)], and modest buffer-gas targets $p_{\text{N}_2} = 50$ kPa require comparable or larger masses $M_{\text{N}_2} \approx 1.9 \times 10^{18}$ kg [Eq. (5)]. The reversible minimum oxygenation work is $E_{\text{min}} \approx 1.2 \times 10^{25}$ J [Eq. (43)], implying $\bar{P}_{\text{min}} \sim 0.38\text{--}3.8$ PW for $t_{\text{build}} = 10^3\text{--}10^2$ yr even before inefficiencies and before filling geochemical sinks (Sec. VIII D).
5. *Mass-efficient warming levers typically trade into sustained maintenance, while one-shot forcing trades into extreme structures.* CIA warming generally couples to continuous H₂ replenishment against escape (Sec. VIII C), and aerosol pathways couple to sustained injection set by residence time (Sec. VI C). Reflector-based TOA forcing scales to continent-class areas for global ΔF_{TOA} . Mechanisms that are mass-efficient (engineered aerosols, H₂ CIA) are typically maintenance-intensive, requiring continuous industrial injection [6]. Mechanisms that are one-shot (mirrors) are structure-mass-intensive (continent-scale areas); and breathable global endpoints require a self-sustaining, civilization-scale industrial base operating for centuries to millennia (Sec. X D).

Taken together, these scalings imply a clear feasibility split. *Regional* habitability gains (E1–E2) are the most credible near- to mid-term path because they scale with *covered area* and local power rather than planet-wide atmospheric inventories: paraterraforming, contained biospheres, and local pressurization/thermal control can be deployed incrementally and deliver meaningful surface utility without requiring exaton-class gases.

By contrast, *global* transformation to E3–E4 is not primarily a “missing greenhouse mechanism” problem. With currently inferred accessible volatiles, an Earth-like Mars (E4) is *not* a century-scale engineering outcome; it becomes credible only under explicit conditions: (i) discovery or delivery of exaton-class volatile inventories (especially an N-bearing buffer gas), (ii) sustained $\mathcal{O}(10^2)$ TW to PW-class power and $\mathcal{O}(10^3)$ Gt yr⁻¹ materials handling for centuries to millennia, and (iii) long-duration climate *control authority* (monitoring + actuation) together with sink/retention management to prevent collapse, escape, and geochemical sequestration.

Even under optimistic assumptions, the reversible oxygenation work alone is $\sim 3 \times 10^{18}$ kWh, which sets an irreducible energy floor before compression, separations, distribution, capital deployment, and long-term maintenance are included. The most technically defensible roadmap is therefore staged: pursue E1–E2 deployments now while using them to demonstrate the industrial primitives—high-capacity power, bulk excavation and processing, global logistics, and closed-loop monitoring/actuation—that are prerequisites for any credible E3–E4 terraforming attempt.

ACKNOWLEDGMENTS

The work described here was carried out at the Jet Propulsion Laboratory, California Institute of Technology, Pasadena, California, under a contract with the National Aeronautics and Space Administration. ©2026. California Institute of Technology. Government sponsorship acknowledged.

-
- [1] C. P. McKay, O. B. Toon, and J. F. Kasting, Making Mars habitable, *Nature* **352**, 489 (1991).
- [2] R. Zubrin and C. P. McKay, Technological Requirements for Terraforming Mars, in *29th Joint Propulsion Conference and Exhibit* (1993) AIAA Paper 93-2005.
- [3] M. J. Fogg, *Terraforming: Engineering Planetary Environments* (SAE International, Warrendale, PA, 1995).
- [4] B. M. Jakosky and C. S. Edwards, Inventory of CO₂ available for terraforming Mars, *Nature Astronomy* **2**, 634 (2018).
- [5] R. Wordsworth, L. Kerber, and C. S. Cockell, Enabling Martian habitability with silica aerogel via the solid-state greenhouse effect, *Nature Astronomy* **3**, 898 (2019).
- [6] S. Ansari *et al.*, Feasibility of keeping Mars warm with nanoparticles, *Science Advances* **10**, eadn4650 (2024).
- [7] International Association for the Properties of Water and Steam (IAPWS), *Revised Release on the Pressure along the Melting and Sublimation Curves of Ordinary Water Substance* (2011), iAPWS Release (R14-08(2011)).
- [8] NASA Office of the Chief Health and Medical Officer, *Habitable Atmosphere (OCHMO-TB-003 Rev A)*, NASA-STD-3001 Technical Brief (2023).
- [9] M. Alexander, *Mars Transportation Environment Definition Document*, Tech. Rep. NASA/TM-2001-210935 (NASA Marshall Space Flight Center, 2001) NTRS Document ID: 20010046858.
- [10] J. C. Stern *et al.*, Evidence for indigenous nitrogen in sedimentary and aeolian deposits from the Curiosity rover investigations at Gale crater, Mars, *Proc. of the National Academy of Sciences of the United States of America* **112**, 4245 (2015).
- [11] National Institute of Standards and Technology (NIST), *NIST Chemistry WebBook, SRD 69: Carbon dioxide (thermophysical properties)*, Online database (2026).
- [12] M. F. Gerstell, J. S. Francisco, Y. L. Yung, C. Boxe, and E. T. Aaltonee, Keeping Mars warm with new super greenhouse gases, *Proc. of the National Academy of Sciences of the United States of America* **98**, 2154 (2001).
- [13] M. M. Marinova, C. P. McKay, and H. Hashimoto, Radiative-convective model of warming Mars with artificial greenhouse gases, *JGR: Planets* **110**, E03002 (2005).
- [14] R. M. Ramirez, R. Kopparapu, M. E. Zuger, T. D. Robinson, R. Freedman, and J. F. Kasting, Warming early Mars with CO₂ and H₂, *Nature Geoscience* **7**, 59 (2014).
- [15] J. Chase, Malcolm W., *NIST-JANAF Thermochemical Tables*, 4th ed. (American Chemical Society and American Institute of Physics for the National Institute of Standards and Technology, Washington, DC, 1998) journal of Physical and Chemical Reference Data, Monograph No. 9.
- [16] J. A. Hoffman *et al.*, Mars Oxygen ISRU Experiment (MOXIE)—Preparing for human Mars exploration, *Science Advances* **8**, eabp8636 (2022), open-access via PubMed Central: PMC9432831.
- [17] NASA, *NASA's Oxygen-Generating Experiment MOXIE Completes Mars Mission* (2023).
- [18] G. J. Taylor, The bulk composition of Mars, *Chemie der Erde – Geochemistry* **73**, 401 (2013).
- [19] J. McSween, Harry Y., G. J. Taylor, and M. B. Wyatt, Elemental composition of the Martian crust, *Science* **324**, 736 (2009).
- [20] B. M. Jakosky *et al.*, Loss of the Martian atmosphere to space: Present-day loss rates determined from MAVEN observations and integrated loss through time, *Icarus* **315**, 146 (2018).
- [21] J. L. Green, J. L. Hollingsworth, D. Brain, V. Airapetian, A. Glocer, A. Pulkkinen, C. Dong, and R. Bamford, A future Mars environment for science and exploration, in *Planetary Science Vision 2050 Workshop* (2017) IPI Contribution No. 1989, abstract #8250.
- [22] D. M. Hunten, The Escape of Light Gases from Planetary Atmospheres, *J. Atmospheric Sciences* **30**, 1481 (1973).
- [23] D. C. Catling and J. F. Kasting, *Atmospheric Evolution on Inhabited and Lifeless Worlds* (Cambridge University Press, 2017) eISBN: 9781139020558.
- [24] F. Forget, R. Wordsworth, E. Millour, J.-B. Madeleine, L. Kerber, J. Leconte, E. Marcq, and R. M. Haberle, 3D modelling of the early martian climate under a denser CO₂ atmosphere: Temperatures and CO₂ ice clouds, *Icarus* **222**, 81 (2013).
- [25] United Nations Environment Programme and International Resource Panel, *Global Resources Outlook 2024*, Tech. Rep. (UNEP / International Resource Panel, Nairobi, Kenya, 2024).
- [26] World Steel Association, *World Steel in Figures 2024*, Tech. Rep. (World Steel Association, Brussels, Belgium, 2024).
- [27] Energy Institute, *Statistical Review of World Energy 2024*, Tech. Rep. (Energy Institute, 2024).